Plant Biotechnology Journal
Open Access

Plant Biotechnology Journal (2023), pp. 1–17 doi: 10.1111/pbi.14186

Simultaneous suppression of lignin, tricin and wall-bound phenolic biosynthesis via the expression of monolignol 4-*O*-methyltransferases in rice

Nidhi Dwivedi[1,2], Senri Yamamoto[3], Yunjun Zhao[1,†], Guichuan Hou[4,†], Forrest Bowling[1], Yuki Tobimatsu[3] and Chang-Jun Liu[1,2,*]

[1]*Biology Department, Brookhaven Nation Laboratory, Upton, New York, USA*
[2]*Feedstocks Division, Joint BioEnergy Institute, Emeryville, CA, USA*
[3]*Research Institute for Sustainable Humanosphere, Kyoto University, Gokasho, Uji, Kyoto, Japan*
[4]*Dewel Microscopy Facility, Appalachian State University, Boone, North Carolina, USA*

Received 27 February 2023;
revised 14 July 2023;
accepted 16 September 2023.
**Correspondence* (Tel 631-344-2966; fax 631-344-3407; email cliu@bnl.gov)
†These authors contributed equally to this work.

Keywords: Monolignol 4-*O*-methyltransferase, lignin, wall-bound phenolics, tricin, 4-*O*-methylated ferulic acid, saccharification.

Summary

Grass lignocelluloses feature complex compositions and structures. In addition to the presence of conventional lignin units from monolignols, acylated monolignols and flavonoid tricin also incorporate into lignin polymer; moreover, hydroxycinnamates, particularly ferulate, cross-link arabinoxylan chains with each other and/or with lignin polymers. These structural complexities make grass lignocellulosics difficult to optimize for effective agro-industrial applications. In the present study, we assess the applications of two engineered monolignol 4-*O*-methyltransferases (MOMTs) in modifying rice lignocellulosic properties. Two MOMTs confer regiospecific *para*-methylation of monolignols but with different catalytic preferences. The expression of MOMTs in rice resulted in differential but drastic suppression of lignin deposition, showing more than 50% decrease in guaiacyl lignin and up to an 90% reduction in syringyl lignin in transgenic lines. Moreover, the levels of arabinoxylan-bound ferulate were reduced by up to 50%, and the levels of tricin in lignin fraction were also substantially reduced. Concomitantly, up to 11 μmol/g of the methanol-extractable 4-*O*-methylated ferulic acid and 5–7 μmol/g 4-*O*-methylated sinapic acid were accumulated in MOMT transgenic lines. Both MOMTs in vitro displayed discernible substrate promiscuity towards a range of phenolics in addition to the dominant substrate monolignols, which partially explains their broad effects on grass phenolic biosynthesis. The cell wall structural and compositional changes resulted in up to 30% increase in saccharification yield of the de-starched rice straw biomass after diluted acid-pretreatment. These results demonstrate an effective strategy to tailor complex grass cell walls to generate improved cellulosic feedstocks for the fermentable sugar-based production of biofuel and bio-chemicals.

Introduction

Grass crops such as rice (*Oryza sativa*), maize (*Zea mays*), wheat (*Triticum aestivum*), sugarcane (*Saccharum* spp.) and sorghum (*Sorghum* spp.) yield not only edible grains but also abundant lignocellulosic materials, such as straw, stover and bagasse, as agricultural residues. Approximately 44 billion tons of such non-wood lignocellulosics are available annually world-wide (Tye *et al.*, 2016), which could potentially produce 491 GL/year bioethanol. Among them rice straw can contribute to 205 GL/year, representing the largest amount from single biomass feedstock (Kim and Dale, 2004). However, as a common obstacle, lignocellulosic utilization is largely impeded by the associated aromatic constituents, including lignin and low-molecular-weight phenolics, within the grass fibers (Halpin, 2019). Lignocellulosic biomass with low lignin content and/or easily removable lignin has been desired (Liu *et al.*, 2014).

Grass stems account for the majority of secondary wall-forming sclerenchyma tissues and the interfascicular fibers that develop thick secondary walls conferring mechanical strength for the upright stem (Coomey *et al.*, 2020). While the architecture of eudicot and monocot cell walls in general is similar, i.e., both consist of a network of cellulose fibers surrounded by a matrix of non-cellulosic polysaccharides and impregnated with lignin, grasses have many special cell-wall features distinct from eudicots and other plants. One of the defining features is the presence of abundant hydroxycinnamates, namely *p*-coumarate (*p*CA) and ferulate (FA). The amounts of these phenolics accumulate up to 3%–4% of dry grass biomass (Hatfield *et al.*, 1999). *p*CA primarily links to lignin through the incorporation of acylated lignin monomers (monolignols) (Karlen *et al.*, 2018), while FA predominantly links to the heteroxylan (arabinoxylan and glucuronoarabinoxylan) through ester linkage between the carboxylic acid group of FA and the primary alcohol on the C5 of arabinosyl side-chain of heteroxylan (Bunzel *et al.*, 2004; de Oliveira *et al.*, 2015). The oxidation of FA in the cell wall generates esterified (dehydro-)diferulate (diFA) and/or oligoferulate bridges, which serve as linkages between two arabinoxylan

Please cite this article as: Dwivedi, N., Yamamoto, S., Zhao, Y., Hou, G., Bowling, F., Tobimatsu, Y. and Liu, C-J. (2023) Simultaneous suppression of lignin, tricin and wall-bound phenolic biosynthesis via the expression of monolignol 4-*O*-methyltransferases in rice. *Plant Biotechnol. J.*, https://doi.org/10.1111/pbi.14186.

polymers. In lignified tissues, esterified FAs on arabinoxylan can also be etherified to lignin polymer units via oxidative radical coupling, forming covalent linkages between hemicellulosic arabinoxylan and lignin, which represents an important mechanism for cell wall reinforcement (Hatfield *et al*., 2016). The esterified FA on arabinoxylan is also considered as a nucleation site of lignification in grass cell walls (Ralph *et al*., 1995). Nevertheless, the FA bridges possess a negative impact on the cell wall digestibility (de Oliveira *et al*., 2015; Grabber *et al*., 1998).

Lignin in both eudicots and monocots is mainly composed of guaiacyl (G) and syringyl (S) units, along with a lower level of *p*-hydroxyphenyl (H) units, which are synthesized via oxidative radical coupling of monolignols, coniferyl alcohol, sinapyl alcohol and *p*-coumaryl alcohol, respectively (Tobimatsu and Schuetz, 2019; Vanholme *et al*., 2010). Although sharing these conventional components with eudicot lignin, grass lignin has several special features, including the incorporations of flavone tricin (Lan *et al*., 2015) and γ-*p*-coumaroylated monolignols such as coniferyl *p*-coumarate and sinapyl *p*-coumarate (Karlen *et al*., 2018) as well as γ-feruloylated monolignols albeit at much lower levels (Karlen *et al*., 2016). Tricin has been revealed to act as a real lignin monomer and incorporate into grass lignin in varying amounts across grass species (del Rio *et al*., 2012; Lan *et al*., 2016b). Its incorporation is mainly established via 4′-*O*-β coupling, thus being proposed to serve as another possible nucleation site for lignification in addition to arabinoxylan-bound FA (Lan *et al*., 2015, 2018).

In monolignol biosynthesis, the aromatic ring of phenolic intermediate is methoxylated at *meta* (3′and/or 5′) positions for the formation of coniferyl alcohol and sinapyl alcohol. The 3′- and 5′-*O*-methylations of benzene ring are catalysed by caffeoyl coenzyme A 3-*O*-methyltransferase (CCoAOMT, EC. 2.1.1.104) and caffeic acid/5-hydroxyferulic acid 3/5-*O*-methyltransferase (COMT, EC. 2.1.1.6), respectively. CCoAOMT preferentially catalyses the methylation of the 3-hydroxyl of 3,4-dihydroxy (caffeoyl) precursors, while COMT prefers 5-hydroxyconiferaldehyde and 5-hydroxyconiferyl alcohol substrates (Guo *et al*., 2001; Parvathi *et al*., 2001). However, many studies reveal that COMT catalyses a broad range of substrates, including not only lignin biosynthetic precursors such as 5-hydroxyconiferaldehyde, 5-hydroxyconiferyl alcohol, caffeoyl aldehyde, caffeoyl alcohol (Osakabe *et al*., 1999; Parvathi *et al*., 2001), but also, flavones luteolin and selgin, leading to the formation of methylated flavone tricin in rice, maize and sorghum (Eudes *et al*., 2017; Fornale *et al*., 2017; Lam *et al*., 2019). Despite the broad substrate range, the activities of both CCoAOMT and COMT are confined to strict regio-specific methylations, i.e., the methylation occurs exclusively at the *meta* (3′ or 5′) -hydroxyl (Bhuiya and Liu, 2010; Osakabe *et al*., 1999; Parvathi *et al*., 2001). The *para*-hydroxyl of lignin monomer is free from methyl etherification and is critically important for radical generation and oxidative polymerization (Bhuiya and Liu, 2010; Davin and Lewis, 2005; Ralph *et al*., 2004). Previously, we have engineered a set of monolignol 4-*O*-methyltransferases (MOMTs) through structure-guided iterative saturation mutagenesis on a parent enzyme, isoeugenol 4-*O*-methyltransferase, an ortholog evolutionarily derived from COMT (Bhuiya and Liu, 2010). The obtained MOMTs confer substantial ability in methylating the *para*-hydroxyl of monolignols. The *para*-hydroxyl methylation deprives the propensity of the modified lignin monomer for further dehydrogenation and incorporation into lignin polymer, which consequently reduces the availability of lignin monomers for polymerization, thus reducing total lignin content or altering lignin composition if a particular type of monolignol is preferentially etherified by MOMTs. One of the mutant variants, MOMT4, which bears four amino acid substitutions (T133L/E165I/F175I/ / H169F) in its active site, effectively catalyses the 4-*O*-methylation of both coniferyl alcohol and sinapyl alcohol, with a slight preference for the latter (Bhuiya and Liu, 2010; Zhang *et al*., 2012). The variant MOMT9, which possesses five additional substitutions (M26H/S30R/V33S/F166W/T319M), however, preferentially etherifies coniferyl alcohol over sinapyl alcohol *in vitro*, due to its significantly reduced substrate binding pocket (Cai *et al*., 2015). The expression of MOMT4 in eudicots (*Arabidopsis* and poplar) significantly impeded lignin formation and/or altered composition, consequently enhanced lignocellulosic digestibility (Cai *et al*., 2016; Zhang *et al*., 2012). Interestingly, the effects of MOMT4 in *Arabidopsis* and poplar on lignin and the related phenylpropanoid biosynthesis were different. The expression of MOMT4 in *Arabidopsis* resulted in the reduction of both G- and S-lignin subunits without alteration in the S/G ratio (Zhang *et al*., 2012), whereas when MOMT4 was expressed in poplar, it drastically reduced S-lignin accumulation without impairing G-lignin subunits and, consequently, drastically reversed the S/G ratio of poplar lignin (Cai *et al*., 2016). These data validate the salient diversity and plasticity of lignin biosynthesis in different plant species and the functional plasticity of MOMTs on lignin formation in different plants. However, this set of engineered MOMTs has not been assessed in grass species. In the present study, we evaluate the effects of not only MOMT4 but also MOMT9 on lignin biosynthesis and cell wall feruloylation in rice. We reveal that the activity of either MOMT variants results in much broader effects in grass than in eudicot species. Not only S- and G-lignin monomers are drastically reduced in rice transgenic lines, the wall-bound *p*CA and FA, and lignin-bound tricin are all dramatically decreased. Concomitantly, significant amounts of novel 4-*O*-methylated phenolics, i.e., the 4-*O*-methylated FA and/or 4-*O*-methylated sinapate derivatives, are accumulated in the methanolic extractable fraction of the MOMT-overexpressing rice. Furthermore, consistent with their *in vitro* catalytic properties, MOMT4 and MOMT9 in the rice transgenic lines exhibit discernible differential effects on the syntheses of lignin and the wall-bound and methanol-soluble phenolics. As a consequence of the cell wall compositional changes, lignocellulosic biomass from MOMT-overexpressing rice shows 15%–30% increases in simple sugar releases after diluted acid pretreatment. These data signify that applying MOMTs could effectively tailor lignin and the related cell wall phenolics biosynthesis in grass species, which allows agricultural residues from grass crops such as rice straw to be more efficiently utilized by mitigating the presence of lignin and cell wall cross-linkers for biofuels production.

Results

Overexpression of MOMT4 and MOMT9 results in the sterility of transgenic rice

To evaluate the effects of MOMT4 and MOMT9 variants on lignin biosynthesis in monocot grasses, the coding sequences of both variants were codon-optimized for rice expression and then placed respectively in an expression cassette driven by the *OsC4H* promoter (Figure 1a). The expression cassettes were transferred into *Oryza sativa* cv. Nipponbare. RT-PCR analysis validated the expression of either transgene in a set of independent T_0 transgenic seedlings (Figure 1b). The selected transgenic plants

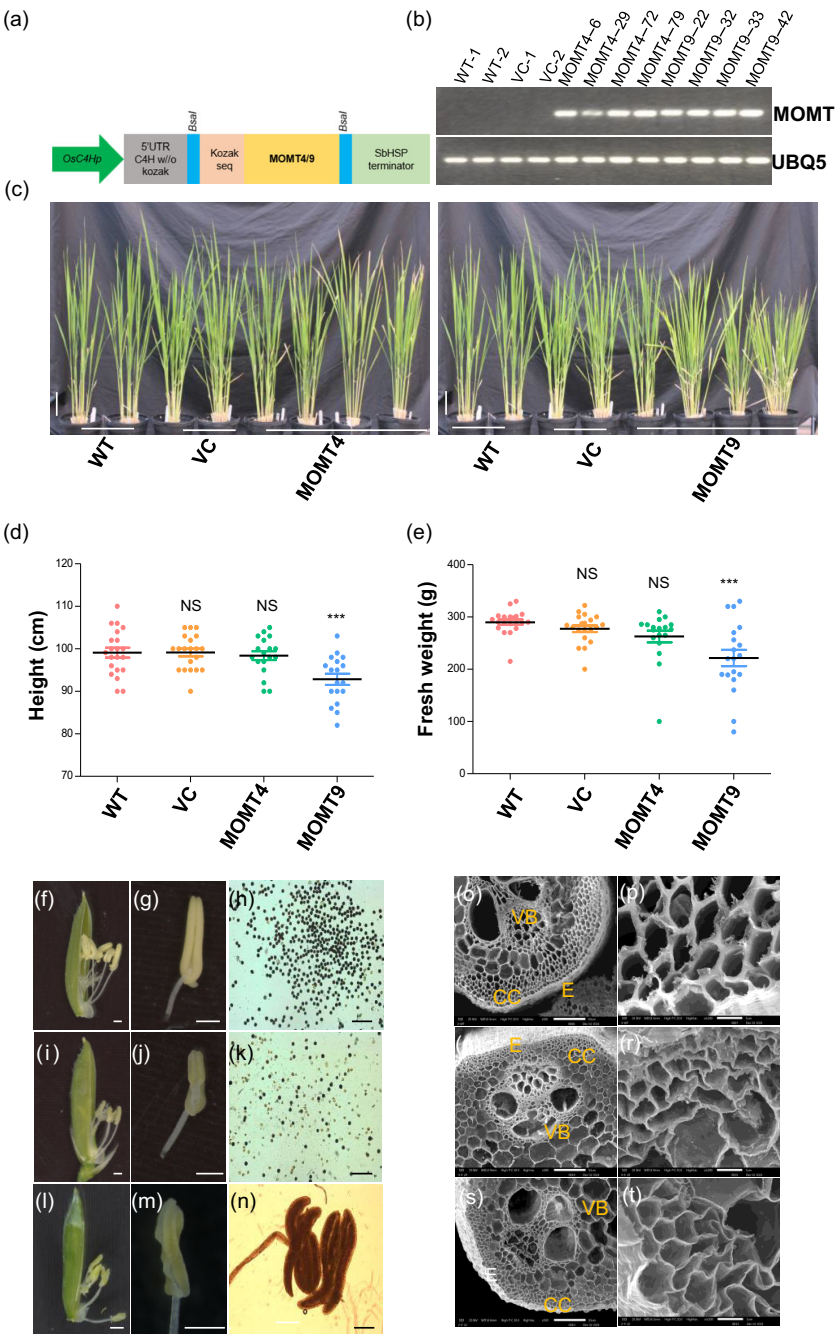

Figure 1 Phenotypic analysis of MOMT4 and MOMT9 transgenic plants. (a) Expression cassette of *MOMT4/9* under *OsC4H* promoter with *OsC4H* 5′ untranslated region, a kozak sequence and a sorghum heat shock protein gene terminator (SbHSP). (b) The RT-PCR analysis of *MOMT4/9* transgene expression in the WT, empty VC, MOMT4, or MOMT9 overexpression lines. Rice ubiquitin 5 gene (UBQ5) was used as the control. (c) Morphology of the regenerated 1.5-month-old MOMT4 and MOMT9 overexpression plants in T_0 generation after first time cutting. Scale bar = 10 cm. (d and e) The measurements of plant height (d) and aerial biomass yield (e). Data are presented as mean ± s.e. (n = 20). Each data point represents individual MOMT4 or MOMT9 transgenic line. *** Indicates statistically significant difference with P <0.001, compared to the WT (one-way ANOVA test; Tukey's multiple-comparison test). (f–n) Floret and anther morphology, and Iodine-potassium iodide staining of mature pollen grains of the WT (f–h), MOMT4 (i–k), and MOMT9 (l–n) overexpression plants. Scale bar = 500 μm in (f–n). Note that MOMT9 anthers did not release any viable pollen grains (n). (o–t) Scanning electron micrographs of transverse sections of the fourth stem internodes of T_0 generation plants after the fourth successive asexual propagation–regeneration, and the enlarged vision of their collenchyma cells of theWT (o, p), MOMT4 (q, r), and MOMT9 (s, t). E, epidermis; CC, collenchyma cells; VB, vascular bundle. Scale bar = 50 μm in (o, q, s) and 5 um in (p, r, t).

were then transferred into soil and grew in a greenhouse condition. Compared to the wild type (WT) and empty vector control (VC) plants, the MOMT4 transgenic lines showed normal growth and displayed no obvious morphological differences in their heights and biomass yields until they approached to the heading stage (Figure 1c–e). However, MOMT9 transgenic lines exhibited a slight dwarfism relative to either the WT or VC controls, with an average 8% reduction in their height and 15%–20% decrease in their fresh biomass yield (Figure 1c–e). When attaining the reproductive stage, both MOMT4 and MOMT9 transgenic lines, however, failed to set seeds. Microscopic examination of their florets discovered that both MOMT4 and MOMT9 transgenic lines developed aberrant white anthers that failed in producing viable mature pollen grains, as indicated by much less or no staining with iodine potassium iodide (IKI) (Figure 1f–n). The IKI stain is widely used for monitoring starch; accumulation of starch in pollen grains is an indicator for pollen maturation (Kosel *et al.*, 2018). Consequently, the impaired (or the lack of) pollen grains caused sterility of the transgenic plants. To rescue and maintain the generated transgenic lines, we adopted asexual propagation. The newly emerged tillers/nodes of the T_0 seedlings were separated from the mature plants and repotted in soil in the greenhouse. Both MOMT4 and MOMT9 transgenic lines were able to regenerate and grow to their mature stage. However, obvious reduction in their heights and the above-ground biomass yields was observed. The calculated above-ground dry biomass yields of the MOTM4 and MOMT9 transgenic lines were 21% and 28% lower, respectively, than those of the

WT/VC plants (Figure S1a–d). To observe the potential anatomic structure alteration of MOMT transgenic plants, transverse sections of the fourth stem internode of rice undergone four times of successive asexual propagation were subjected to scanning electron microscopic observation. The images showed that MOMT4 and MOMT9 over-expression plants in general developed normal vascular bundles in their developing stems as did the WT and VC plants, but overall, the cell wall thickness of the vessel, tracheid, and bundle sheath cells and that of the cortical fibre (collenchyma) cells appeared reduced, compared to the WT and VC samples; and some of the vessel cells appeared slightly deformed or collapsed (Figure 1o–t).

MOMT transgenic lines accumulate novel soluble phenolics

Metabolic profiling of methanolic extracts from 1.5-month-old rice aerial parts, including stems and leaves, via liquid chromatography-mass spectrometry (LC-MS), revealed four unique metabolites (P1–P4) that appeared in both MOMT4 and MOMT9 transgenic lines but were absent in the WT and VC control plants (Figure 2a–d and Figures S2 and S3). The metabolite P1 showed a UV spectrum analogous to that of FA but with a molecular ion $[M–H]^-$ at *m/z* of 429 and a corresponding fragment ion at *m/z* of 207 that indicates the presence of a 4-*O*-methylated FA core structure. The neutral loss of *m/z* 222 (162+60) between the molecular ion and the 4-*O*-methylated FA fragment ion suggests P1 is a 4-*O*-methylated FA glucose ester conjugate (Figure 2e). Similarly, the metabolite P2 showed a UV spectrum similar to sinapate but with a molecular ion at *m/z* 459 and a fragment ion at *m/z* 237, indicating a 4-*O*-methylated sinapate glucose conjugate (Figure 2f). Correspondingly, the 4-*O*-methylated FA (P3) and 4-*O*-methylated sinapate (P4) aglycones were detected along with their glucose conjugates (Figure 2a–d and Figure S2a–d). HCl-digestion of the extracts completely converted the glucose conjugates P1 and P2 into their corresponding aglycones P3 and P4, respectively (Figure S2b–d). The accumulation levels of the 4-*O*-methylated FA were about 8–11 μmol/g dry-weight and those of the 4-*O*-methylated sinapate aglycone were 5–7 μmol/g, respectively, in MOMT4 over-expression plants (Figure 2g). Interestingly, while MOMT9 transgenic lines accumulated similar levels of 4-*O*-methylated FA as those accumulated in MOMT4 transgenic plants, the levels of 4-*O*-methylated sinapate were significantly lower, compared to those accumulated in MOMT4 over-expression plants, showing only 0.35–0.45 μmol/g dry-weight (Figure 2g). This was even more obvious in the leaf extracts where the 4-*O*-methylated FA was abundantly detected with up to 11.5–16 μmol/g fresh weight, while 4-*O*-methylated sinapate was nearly absent in the MOMT9 transgenic plants (Figure S3). These results indicate that while both MOMT variants function properly as the *para*-*O*-methyltransferase in grass rice, consistent with our previous biochemical study, MOMT9 preferentially methylates G precursor (FA) over S precursor (sinapate), leading to the less formation of the 4-*O*-methylated sinapate in its overexpression rice. This is because MOMT9 possesses a significantly smaller substrate-binding pocket in comparison with MOMT4, which hinders the binding of the bulkier S-type substrates (Cai *et al*., 2015).

Apart from the accumulation of the novel 4-*O*-methyalted phenolics, LC-MS profiling also revealed up to 80% reduction of the methanolic extractable tricin (P5) in both MOMT4 and MOMT9 over-expression lines, compared to that in the WT or VC lines (Figure 2a–d,g and Figure S2a,d,e), suggesting the expression of MOMT variants somehow affects flavone tricin biosynthesis.

Overexpression of MOMT4 and MOMT9 suppresses the accumulation of wall-bound hydroxycinnamates

Grass walls contain significant amounts of hydroxycinnamates, such as FA and *p*CA. These ester-linked hydroxycinnamates can be released by mild alkaline hydrolysis (Figure 3a). After 4N NaOH treatment, the cell wall residues (CWRs) of the 1.5-month-old aerial part of WT rice released approximately 1.4–1.6 μmol/mg FA and 0.7–0.9 μmol/mg *p*CA. However, the amount of FA released from the cell walls of both MOMT4 and MOMT9 transgenic plants was reduced by up to 50%; and *p*CA was reduced by more than 57% in MOMT4 transgenic lines and about 40% in MOMT9 overexpression lines, compared to the WT (Figure 3b,c). The amount of FA dimers with sum of all the potential cross-linkages showed up to 30% reduction in MOMT4 and MOMT9 over-expression lines, compared to the WT and VC plants (Figure 3d). In addition to the wall-bound FA and *p*CA, one uncharacterized compound with a molecular ion at *m/z* of 181 but with a similar UV spectrum as *p*CA was also significantly reduced in the cell walls of MOMT4 and MOMT9 over-expression lines (Figure 3e). These data indicate that the expression of MOMTs suppresses the incorporation of wall-bound phenolics.

Mild acidolysis preferentially cleaves glycosidic linkages of arabinosyl-(1→3)-xylan in glucouronoarabinoxylan chains, therefore, enabling to detect and quantify the arabinoxylan-bound hydroxycinnamate conjugates in grass cell walls (Eugene *et al*., 2020; Lapierre *et al*., 2019). To further examine the potential effects on hydroxycinnamates (FA and/or *p*CA) specifically linked to arabinoxylan, mild acidolysis with 50 mM trifluoroacetic acid (TFA) was performed on the CWRs of both MOMT4 and MOMT9 transgenic lines. LC-MS analysis of the TFA-treated samples revealed several putative dimeric or oligomeric sugars (P1–P6) released from the cell walls (Figure S4). Among them, the product P1 displayed a molecular ion $[M–H]^-$ at *m/z* 295.08 and the diagnostic fragment ion of *p*CA at *m/z* of 163.04, as well as an ion at *m/z* 235, which represents the presence of Ara-*p*CA (Figure S4b). The co-eluted product P2 showed a molecular ion $[M–H]^-$ at *m/z* 457.13 and corresponding fragment

Figure 2 Accumulation of methanolic soluble phenolics in MOMT transgenic rice. (a–d) A portion of UV-LC-MS profile of undigested methanolic phenolic extracts from 1.5-month-old aerial tissues of the WT (a), VC (b), MOMT4 (c), and MOMT9 (d) over-expression plants. P1 is tentatively identified as 4-*O*-methylated feruloyl glucose derivative; P2 is 4-*O*-methylated sinapoyl glucose derivative; P3, 4-*O*-methylated ferulic acid aglycone; P4, 4-*O*-methylated sinapic acid aglycone; P5, tricin; IS, internal standard. (e and f) The corresponding UV, mass and tandem mass (MS2) spectra of the metabolite P1 (e) and P2 (f), respectively. (g) The accumulation levels of the detected phenolics in aerial tissue of MOMT4 or MOMT9 overexpression plants after 2N HCl digestion. Data are presented as the mean ± s.e. from two biological replicates with four technical repeats for the WT and VC plants and four technical repeats for MOMT4 and MOMT9 independent transgenic lines. *** indicates statistically significant difference with $P < 0.001$, compared to the WT (one-way ANOVA test; Tukey's multiple comparison test). ND – not detectable. DW, dry weight.

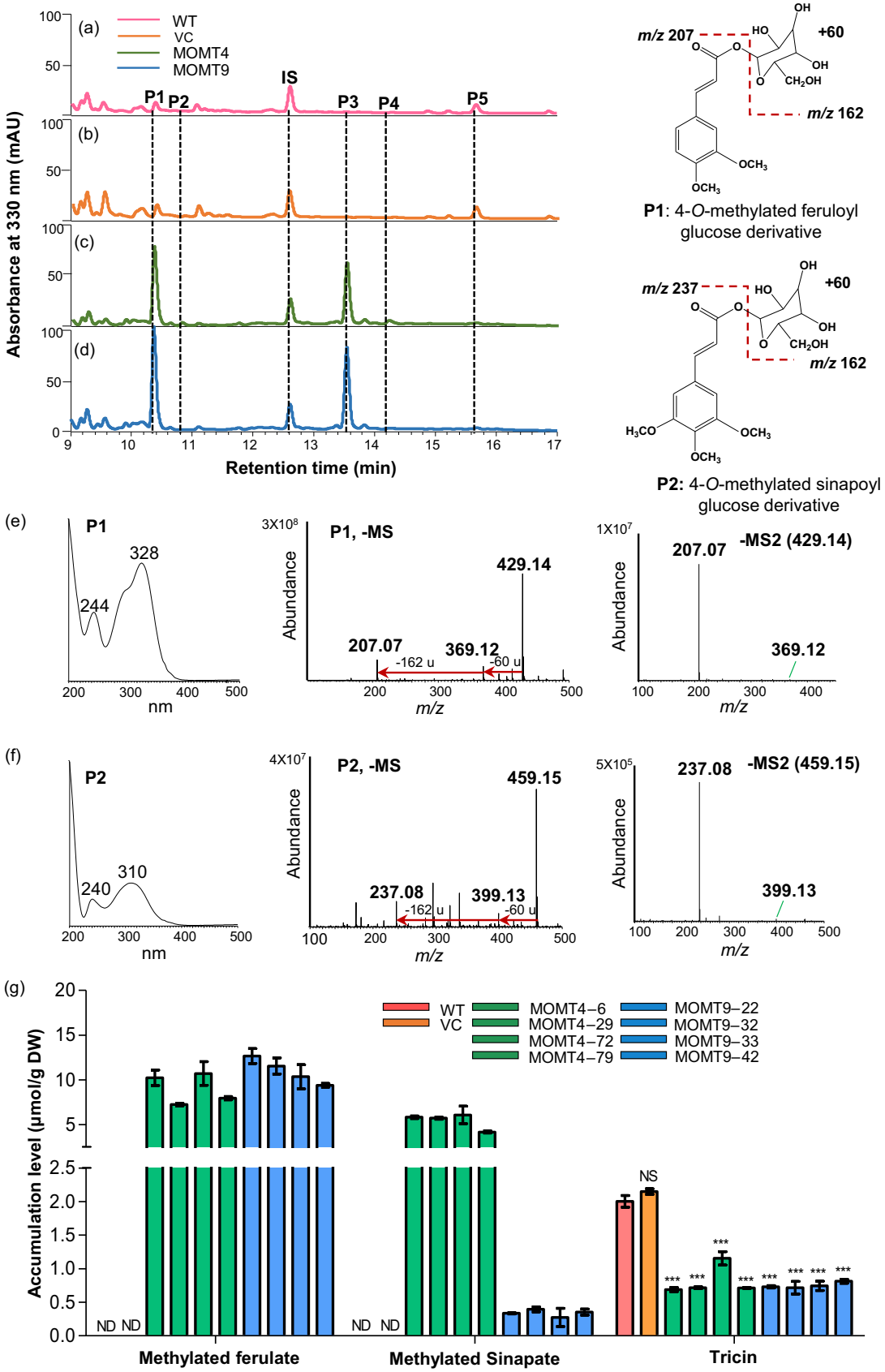

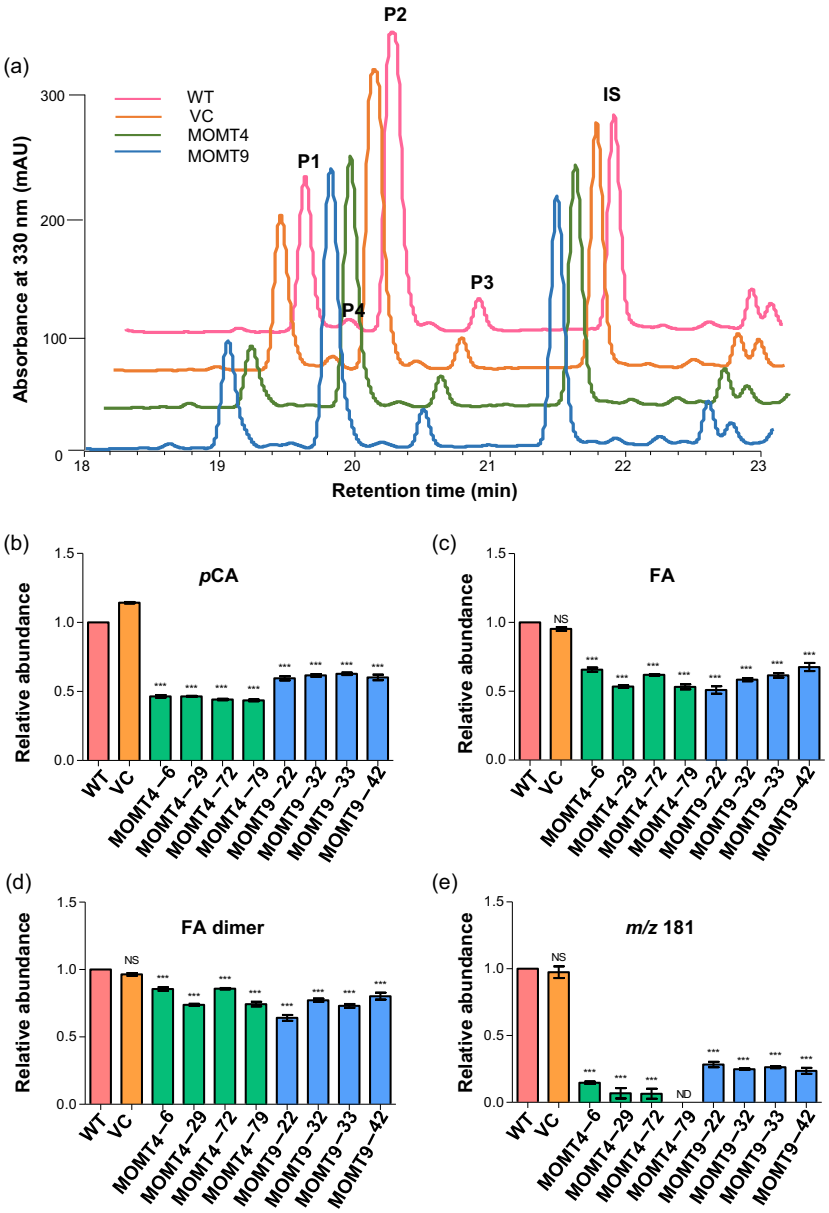

Figure 3 Wall-bound hydroxycinnamates released by alkaline treatment. (a) A portion of UV-LC-MS profile of wall-bound phenolic extracts from cell wall residues of aerial tissues of 1.5-month-old of WT, VC, MOMT4 and MOMT9 overexpression rice. P1, *p*-coumarate (*pCA*); P2, ferulate (FA); P3, ferulate dehydrodimer; P4, unknown peak with *m/z* 181. IS, internal standard. (b–e) Relative abundance of wall-bound phenolics in MOMT4 and MOMT9 overexpression lines, compared to the WT; (b) *p*CA, (c) FA, (d) FA dimers and (e) Unknown peak with *m/z* 181. Quantifications of *p*CA, and FA and unknown compound were based on their UV absorption peak area, while quantification of FA dimers was based on the extracted ion abundance at *m/z* 385.09. The average amount detected in the WT was set as 1. Data are presented as the mean ± s.e. from two biological replicates with four technical repeats for the WT and VC plants and four technical repeats for individual MOMT4 and MOMT9 overexpression lines. *** indicates statistically significant difference with $P < 0.001$, compared to the WT (one-way ANOVA test; Tukey's multiple comparison test). NS, not significant. ND, not detectable.

ion 265.07 and 193.05, the diagnostic fragment ion of FA, therefore being defined as Xyl-Ara-FA (Figure S4c). The product P3 had a molecular ion at *m/z* of 325.09 and fragment ion at *m/z* of 265.07 and 193.05 that represent the Ara-FA (Figure S4d). In addition, a minor peak P4 showed *m/z* of 649.18/589.18 (Figure S4e), which is consistent with the previous assignment of Ara-diFA-Ara (de Souza *et al.*, 2018). The products P5 and P6 represent *p*CA and FA aglycones, respectively (Figure S4). All those compounds showed obvious decreases in the MOMT4 and MOMT9 transgenic plants (Figure S4a). After saponification of the mild acidolysis products, the phenolics linked to the sugar residues were completely released and were confirmed as *p*CA, FA, or diFA (Figure 4a). Quantification of those phenolics revealed that the distribution of FA on arabinoxylan was reduced by 50%–60% in both MOMT4 and MOMT9 overexpression lines, while the distribution of *p*CA was reduced by up to 30% in MOMT4 overexpression plants, it was even slightly increased in MOMT9 overexpression plants (Figure 4a,b), suggesting differential impacts of two MOMT variants on *p*CA incorporation. These results indicate that the expression of MOMTs impairs the phenolics esterified to the polysaccharide fractions in the rice cell walls.

Overexpression of MOMT4 and MOMT9 alters cell wall polymer composition

MOMTs specifically modify the *para*-hydroxyl of monolignols, thereby reducing the availability of lignin precursors incorporated into lignin polymer (Cai *et al.*, 2016; Zhang *et al.*, 2012). The expression of them in planta is thus expected to suppress lignin formation and/or alter lignin structure. With the prepared ethanol extractive-free, de-starch and de-protein CWRs, we determined lignin content using the acetyl bromide method (Foster *et al.*, 2010a), which suggested up to a 30% reduction in the total lignin content of either MOMT4 or MOMT9 over-expression plants, compared to the WT or VC plants (Figure 5a). Furthermore, lignin monomeric composition was determined via

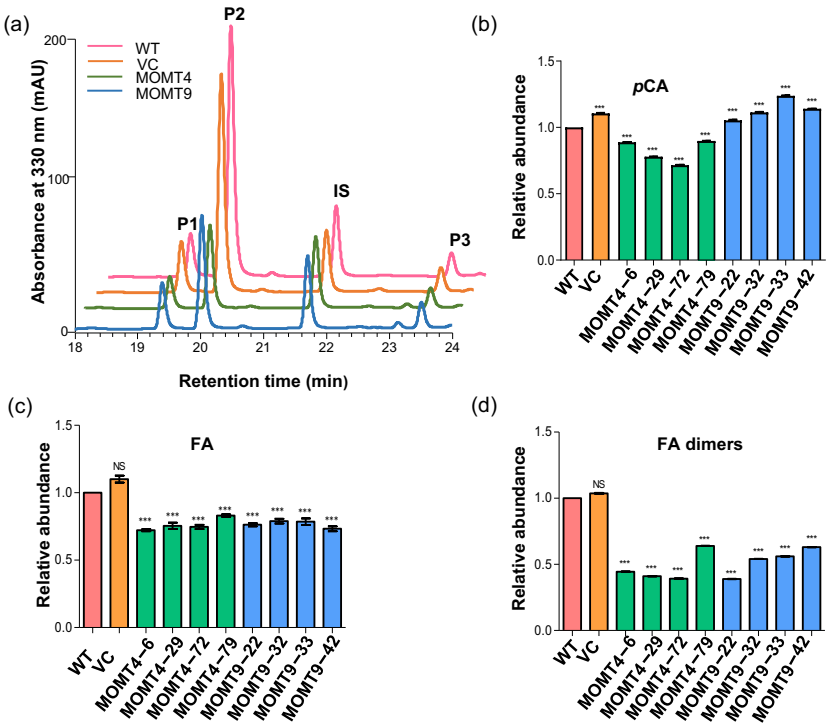

Figure 4 Wall-bound hydroxycinnamates released by mild acidolysis. (a) A portion of UV-LC-MS profile of phenolic extracts recovered after trifluoroacetic acid (TFA)-mediated mild acidolysis and saponification of cell wall residues from 1.5-month-old WT, VC, MOMT4 and MOMT9 overexpression plants. P1, *p*-coumarate (*p*CA); P2, ferulate (FA); P3, ferulate dehydrodimer. IS, internal standard. (b–d) Relative abundance of the phenolics *p*CA (b), FA (c) and FA dimers (d) released from the arabinoxylan-bound in MOMT4 and MOMT9 overexpression lines, compared to the WT. Quantifications of *p*CA and FA were based on their UV absorptive peak area, while quantification of FA dimers was based on the extracted ion abundance at *m/z* 385.09. The average amount detected in the WT was set as 1. Data are represented as mean ± s.e. from two biological replicates with three technical repeats for WT and VC plants and three technical repeats for individual MOMT4 and MOMT9 overexpression lines. *** indicates statistically significant difference with $P < 0.001$, compared to the WT (one-way ANOVA test; Tukey's multiple comparison test). NS, not significant.

analytical thioacidolysis, which selectively cleaves the major β-*O*-4 aryl ether linkages in lignin polymer and releases lignin-derived monomeric products (Rolando *et al.*, 1992). As anticipated, both G- and S-lignin-derived monomers were drastically reduced in MOMT4 and MOMT9 overexpression plants. Approximately 60%–75% G monomers and up to 93% S monomers were reduced in MOMT4 overexpression lines; while about 58%–66% of G and ~77% of S were decreased in MOMT9 overexpression plants, compared to the WT control plants (Figure 5b). Consequently, the thioacidolysis-derived S/G lignin unit ratio was substantially altered from ~0.66 in the WT to ~0.2 in the MOMT4 lines and ~0.5 in the MOMT9 lines (Figure 5c). These results again confirm that both MOMT variants function in rice and substantially impair lignin biosynthesis; nevertheless, MOMT4 more affects the S-type monomers (sinapyl alcohol and sinapyl *p*-coumarate) than the G-type monomers (coniferyl alcohol), while MOMT9, with its smaller substrate binding pocket (Cai *et al.*, 2015), shows a disfavoured modification on the S-type monomers relative to MOMT4.

To further dissect the potential changes in lignin structure, two-dimensional (2D) heteronuclear single-quantum coherence (HSQC) nuclear magnetic resonance (NMR) analysis was conducted on the ball-milled CWRs prepared from the selected MOMT4 and MOMT9 transgenic lines, and WT and VC control plants by the whole-cell-wall dissolution method using the dimethylsulfoxide-d_6/pyridine-d_5 solvent system (Kim and Ralph, 2010). The HSQC NMR spectra of the rice cell walls displayed typical contour signals from lignin, polysaccharides and cell-wall-bound hydroxycinnamates (Figure 6, Figure S5 and Table S1). For a semi-quantitative examination of the relative proportions of the cell wall components, we performed volume integration analysis of the well-resolved aromatic signals from lignin and *p*-hydroxycinnamate units (Figure 6a) and sugar anomeric signals from cell wall polysaccharide units (Figure 6b); the reported signal intensity data are the relative intensities normalized based on the sum of the integrated signals, reflecting the proportional amount of each component in the rice cell walls (see Materials and Methods for details; Figure 6c,d).

Notably, the S and G lignin aromatic signals (**S** and **G**, respectively) were drastically reduced in both MOMT4 and MOMT9 transgenic lines (Figure 6a). The volume integration analysis determined that G signals were reduced by 35%–54% in the spectra of both MOMT4 and MOMT9 transgenic cell walls, whereas S signals were reduced more prominently by 76%–79% in the spectra of the MOMT4 transgenic cell walls and about 61%–65% in the spectra of the MOMT9 transgenic cell walls as compared to those in the spectra of the WT and VC control cell walls (Figure 6c,d). These NMR data indicated that, in agreement with the lignin content and composition data obtained by the chemical methods (Figure 5), the monolignol-derived S and G lignin units are substantially reduced in the MOMT transgenic lines with more prominent reductions in S lignin units over G

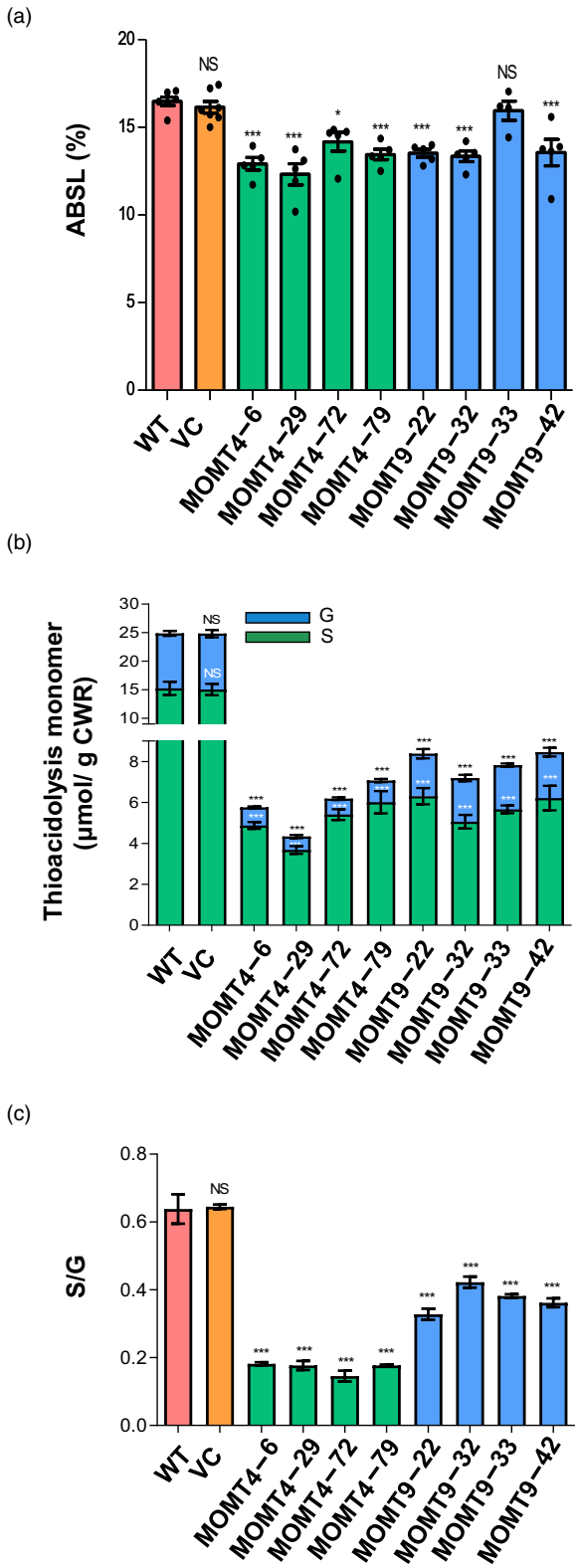

Figure 5 Total lignin content and composition of aerial tissues of MOMT transgenic plants. (a) Acetyl bromide soluble lignin (ABSL) content in the cell wall residues (CWRs) of 1.5-month-old rice aerial tissues of the WT, VC, MOMT4 and MOMT9 overexpression lines. (b) The monomers released by thioacidolysis. G, guaiacyl unit; S, syringyl unit. (c) Corresponding S/G monomer ratio. Data are represented as mean ± s.e. from two biological replicates with three or more technical repeats in the WT and VC and three or more technical repeats from each individual MOMT4 and MOMT9 overexpression lines. * indicates statistically significant difference with $P < 0.05$; *** indicates statistically significant difference with $P < 0.001$, compared to the WT (one-way ANOVA test; Tukey's multiple comparison test). NS, not significant.

lignin units in the MOMT4 transgenic lines than in the MOMT9 transgenic lines.

In addition to the reductions in the monolignol-derived lignin signals, the aromatic signals from the cell-wall-bound FA (**F**) and *p*CA (**P**) (Figure 6a) were also clearly reduced, by up to 55%, in the spectra of the MOMT transgenic cell walls compared to those in the spectra of the WT and VC cell walls (Figure 6c,d), which was also in line with the cell wall-bound hydroxycinnamate data obtained by the chemical analysis (Figures 3 and 4). Furthermore, notably, the lignin-bound flavone tricin signals (**T**) (Figure 6a) were reduced by 19%–32% in the spectra of the MOMT9 transgenic cell walls, and by 42%–55% in the spectra of the MOMT4 transgenic cell walls (Figure 6c,d). Hence, along with monolignols and hydroxycinnamates, the incorporation of the tricin monomer into lignin is impeded in the MOMT transgenic lines.

While the considerable reductions occurred in the lignin, hydroxycinnamate and tricin signals in the cell wall spectra of the MOMT transgenic lines, the slight increases of the polysaccharide anomeric signals were observed (Figure 6b). Based on the volume integration analysis, the glucose signals (**Gl**) were most prominently increased, by 14%–18%, in the spectra of the MOMT transgenic cell walls in comparison with the WT and VC control spectra, although less prominent proportional increases (by 2%–9%) in the xylose (**X**, **X′** and **X″**) and arabinose (**A**) signals were also observed (Figure 6c,d). Nevertheless, chemical analyses using the conventional neutral sugar analysis methods (Foster *et al.*, 2010b) (Dubois *et al.*, 1956) did not detect statistically significant differences in the sugar contents between the cell walls of the MOMT transgenic lines and the WT and VC control plants (Figure S6).

MOMT4 and MOMT9 exhibit substrate promiscuity to a range of phenolics

The above soluble phenolics and cell wall structural analyses of the MOMT4 and MOMT9 transgenic plants showed the reduced accumulations of soluble and wall-bound tricin and hydroxycinnamates along with the monolignol-derived lignin units, which promoted us to reconfirm the substrate specificities of MOMT4 and MOMT9. Accordingly, hydroxycinnamates *p*CA, FA and sinapate, flavanone naringenin, and flavones tricin, luteolin and chrysoeriol were tested as the potential substrates, in comparison with monolignols (coniferyl alcohol and sinapyl alcohol) in the specific activity assay. While MOMT4 and MOMT9 showed prominent catalytic activity to monolignols (coniferyl alcohol and/or sinapyl alcohol), both enzymes displayed low but discernible activities to hydroxycinnamates and flavones (Table 1). Specifically, MOMT4 exhibited about 5% catalytic activity to FA or luteolin, compared to that to coniferyl alcohol; while MOMT9, as our previous detection (Liu and Cai, 2017) displayed nearly comparable catalytic activity to FA as to coniferyl alcohol. In addition, it also showed detectable activity to tricin (~9%) and

chrysoeriol (~4.5%) in comparison with its activity to coniferyl alcohol (Table 1).

Expression of MOMT 4 and 9 improves the cell wall digestibility

Lignin and cell wall-associated hydroxycinnamates are proposed to be negatively related to the enzymatic digestibility of grass cell walls (de Oliveira *et al*., 2015). The significant decreases in lignin and wall-bound hydroxycinnamate contents of both MOMT4 and MOMT9 transgenic rice promoted us to further assess their biomass processability. The de-starched CWRs from MOMT4 and MOMT9 overexpression plants were pre-treated with a mild acid (1.2% v/v H_2SO_4), and the pretreated slurry after neutralization was then directly digested with Cellic CTec2, a blend of cellulases, β-glucosidases and hemicellulases. The yield of released glucose exhibited 15%–30% increase in the MOMT4 CWR samples and 10%–15% increase in MOMT9 overexpression samples in comparison with those of WT and VC CWRs (Figure 7a). When pretreated with an alkaline solution (0.25% w/v NaOH), the de-starched CWRs of MOMT4 overexpression plants also exhibited 6%–10% increase in the simple glucose release (Figure 7b). However, the saccharification yield did not exhibit significant enhancement when the raw biomass of most of the transgenic lines was subjected to the acid or alkaline pre-treatments (Figure S7).

Discussion

Grass lignocelluloses represent an abundant renewable biomass source for chemical pulping and fermentable sugar-based applications such as biofuel and biochemical productions (Tye *et al*., 2016; Umezawa, 2018). However, as the common obstacle, lignin present in the grass cell walls confers significant recalcitrance to enzymatic hydrolysis (Moore and Jung, 2001). Moreover, the cell wall matrix of grass is much more complicated than that in eudicots and gymnosperms, featuring the presence of the cell-wall-cross-linking FA and the lignin decorations by *p*CA and flavone tricin (Ralph *et al*., 2019). These complexities render substantial difficulties in optimizing grass lignocellulosics for agro-industrial applications.

The expression of either MOMT4 or MOMT9 in rice resulted in drastic reduction of both lignin and wall-bound phenolics; concomitantly, a large quantity of methanolic extractable 4-*O*-methylaled phenolics were produced (Figures 2, 3, 5 and 6). These results demonstrate the effectiveness and robustness of both MOMTs in tailoring grass cell wall chemical and structural properties. The expression of MOMTs in rice led to a drastic reduction of both G and S lignin units, which differs from what occurred when MOMT4 was expressed in eudicot poplar, where S lignin unit was predominantly suppressed (Cai *et al*., 2016). This discrepancy might reflect the diversity and plasticity of the phenylpropanoid and lignin biosynthesis among different plant species. Poplar wood particularly its fibre walls enriches S-lignin with S:G ratio around 2 (Zhao *et al*., 2021), while lignin of grass species contains approximately equal amount of G and S subunits with S:G ratio around 0.6–0.7 (Lam *et al*., 2017, 2019). In addition, the promoters used to drive MOMT transgene expression in poplar and rice are also different; in the former, it was a French bean PAL2 gene promoter, while in the latter a rice C4H gene promoter was adopted, which might lead to differential spatiotemporal expression patterns of MOMT transgenes, ultimately result in different chemical phenotypes. Furthermore, two tested MOMT variants exhibit different effects on lignin and phenolic biosynthesis in planta. MOMT4, which favours methylating the S-type sinapyl alcohol over the G-type coniferyl alcohol *in vitro* (Bhuiya and Liu, 2010; Zhang *et al*., 2012), suppresses more S lignin deposition in transgenic rice, resulting in large reductions in the S/G lignin ratios as determined by both thioacidolysis (Figure 5c) and 2D NMR (Figure 6c), whereas expressing MOMT9, a variant that more prefers modifying G monomers over S monomers in vitro due to its smaller substrate binding pocket (Cai *et al*., 2015), leads to a less prominent effect on the S/G lignin ratio reductions (Figures 5c and 6c), and concomitantly the sole production of the soluble 4-*O*-methylated FA-derived metabolites (Figure 2). These results demonstrate that both MOMT variants function properly in grass species and are in line with their in vitro structural and catalytic properties.

The expression of both MOMTs not only suppressed lignin biosynthesis but also drastically reduced wall-bound FA and *p*CA (Figure 3). The FA and *p*CA esters, particularly the FA-arabinoxylan esters, have been demonstrated to be involved in radical coupling reactions to cross-link cell wall polysaccharide (arabinoxylan) and lignin polymer chains. The resulting arabinoxylan-FA-arabinoxylan and arabinoxylan–FA–lignin complexes represent the key structures that stabilize grass cell walls and maintain cell wall rigidity (Hatfield *et al*., 2016). In vitro assays suggested that the wall-bound FA is negatively correlated with cell wall digestibility (de Oliveira *et al*., 2015). Suppression of wall-bound FA in *Setaria viridis* via the downregulation of a BAHD acyltransferase that potentially functions for conjugating FA to arabinoxylan significantly improved biomass saccharification efficiency (de Souza *et al*., 2018). The mild acidolysis, a procedure for determining the relative acylation of grass arabinoxylan (Eugene *et al*., 2020; Lapierre *et al*., 2019), revealed about 60% reduction of arabinoxylan-bound FA in the cell walls of the MOMT transgenic lines (Figure 4). Such drastic loss of the arabinoxylan-bound FA expectedly could result in the decrease of cross-links between the matrix heteroxylan and lignin polymer chains, contributing to the improvement of enzymatic cell wall digestibility.

Significant suppression of the wall-bound phenolics, particularly the polysaccharide-linked FA, in the MOMT overexpression lines is somehow unexpected. The formation of wall-bound hydroxycinnamates is catalysed by particular BAHD family acyltransferases that transfer FA or *p*CA moieties from their corresponding CoA thioesters to the acceptors (e.g., arabinose and/or monolignols); then the conjugates are incorporated into polysaccharides or lignin (Bartley *et al*., 2013; de Souza *et al*., 2018; Li *et al*., 2018; Petrik *et al*., 2014; Withers *et al*., 2012). While MOMTs possess strict regiospecificity, *viz*. specifically catalysing *para*-hydroxyl methylation of aromatic ring, they show a certain extent of substrate promiscuity and recognize a range of small molecule phenolics, including FA in addition to the monolignols (Table 1). Therefore, one possibility is that MOMTs, when over-accumulated in planta, also methylate the accessible hydroxycinnamic acids besides monolignols. The resulting 4-*O*-methoxycinnamic acids are likely unable to be efficiently catalysed by the endogenous 4-coumaroyl CoA ligases to transform to the active CoA thioesters, or the produced 4-*O*-methoxycinnamoyl CoAs can't be further utilized by BAHD family acyltransferases. Consequently, the availability of FA incorporating into the cell wall fraction is restricted (See the depiction in Figure S8). This assumption is consistent with the observation

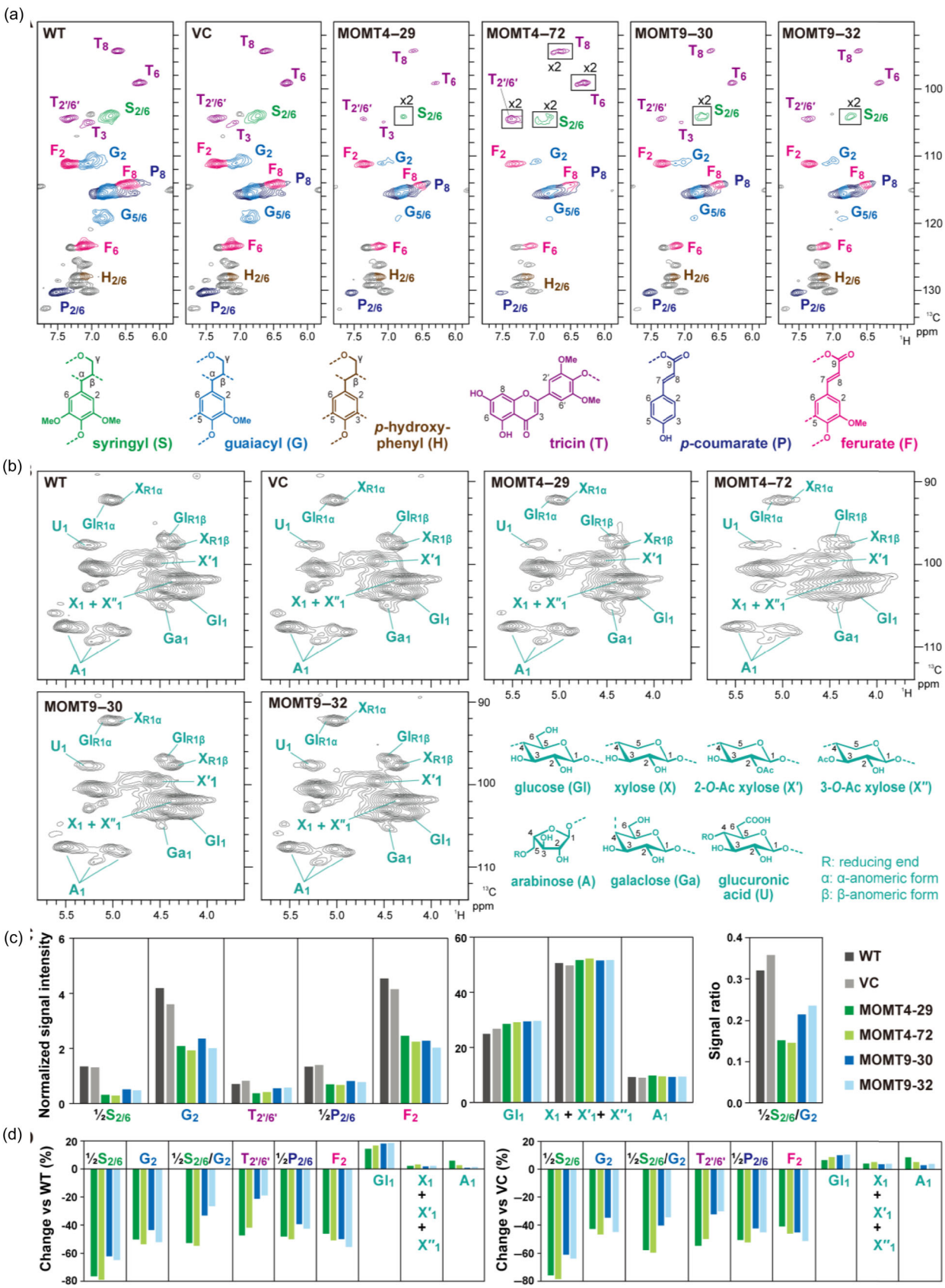

Figure 6 Two-dimensional NMR analysis of whole stem cell walls from MOMT transgenic rice plants. (a and b) Aromatic (a) and oxygenated aliphatic (b) sub-regions of $^{1}H–^{13}C$ short-range correlation (HSQC) NMR spectra are shown. Contour coloration matches that of lignin substructures shown in each panel. Boxes labeled with ×2 indicate regions with scale vertically enlarged for 2-fold. Full spectra are shown in Figure S5. (c) Normalized signal intensities and ratios of major lignin, hydroxycinnamate, and polysaccharide units expressed as percentages of the sum of the listed signals ($½S_{2/6} + G_2 + ½P_{2/6} + F_2 + ½T_{2'/6'} + GI_1 + X_1 + X'_1 + X''_1 + A_1 = 100$). (d) Percentage changes of the normalized signal intensities and ratios of the major cell wall units in the spectra of MOMT transgenic lines compared to those in the wild-type (WT) and VC lines.

Table 1 Specific activities of MOMT4 and MOMT9 with different phenolic substrates

	Specific activity (nmol/mg/min)	
Substrate	MOMT4	MOMT9
Coniferyl alcohol	63.42 ± 3.48 (100)†	59.01 ± 5.20 (100)†
Sinapyl alcohol	59.42 ± 1.44 (93.10)	9.14 ± 1.00 (15.45)
Ferulic acid	3.72 ± 0.24 (5.83)	55.31 ± 2.32 (93.85)
Sinapic acid	3.34 ± 0.04 (5.23)	3.83 ± 0.24 (6.50)
Chrysoeriol	0.09 ± 0.01 (0.14)	2.71 ± 0.10 (4.58)
Luteolin	3.59 ± 0.13 (5.62)	0.77 ± 0.03 (1.31)
Tricin	0.49 ± 0.16 (0.77)	5.50 ± 0.02 (9.30)
Naringenin	nd	nd
p-Coumaric acid	nd	nd

The specific activity was measured from the reaction with 500 μM S-adenosyl *L*-methionine and 500 μM phenolic substrate at 30 °C for 10 (or 20) min. The data represent the mean ± s.e. of three experimental replicates.

nd, not detectable.

†Data in parentheses represent the relative activity compared to that MOMT 4 or 9 to coniferyl alcohol.

that both MOMT4 and MOMT9 exhibit detectable activities in methylating the examined FA (Table 1) and of the hyper-accumulation of the methanolic soluble 4-*O*-methylated FA metabolites in the MOMT transgenic plants (Figure 2). Interestingly, along with FA, the cell-wall-bound *p*CA was largely reduced in the MOMT transgenic plants (Figures 3 and 6) despite the 4-*O*-methylation activity towards *p*CA was barely detectable for MOMTs (Table 1). Given that cell-wall-bound *p*CA in grass cell walls is mainly originated from the incorporations of monolignol-*p*CA conjugates (i.e., sinapyl *p*-coumarate) in lignification (Karlen *et al.*, 2018), it is plausible that the reductions of cell-wall-bound *p*CA in the MOMT transgenic lines are mainly due to the disruptions of the incorporations of monolignol-*p*CA conjugates via 4-*O*-methylations of their monolignol moieties by MOMTs. Alternatively, the 4-*O*-methylation of monolignols might divert a large portion of metabolic flux away from the phenylpropanoid–lignin pathway, resulting in the overall reduction in the amount of both lignin biosynthetic precursors and pathway intermediates, including hydroxycinnamates, such as *p*CA and FA, thus limiting the availability of monomeric precursors for lignin polymerization and for wall-bound phenolic ester synthesis.

The productions of soluble 4-*O*-methylated FA and 4-*O*-methylated sinapate glucose esters suggest that rice has a versatile phenolic ester biosynthetic pathway. In *Arabidopsis*, a hydroxycinnamaldehyde dehydrogenase (aldehyde dehydrogenase, ALDH, also known as REF1) converts lignin precursors coniferaldehyde and sinapaldehyde into the corresponding hydroxycinnamates, FA and sinapate, respectively, which can then be transformed into the corresponding esters via conjugation with glucose, malate, or choline through the activities of specific glycosyltransferases and/or acyltransferases (Nair *et al.*, 2004). This intrinsic phenolic ester biosynthetic pathway exhibits considerable flexibility and able to accommodate and transform the 4-*O*-methylated monolignols or their aldehydes into the corresponding 4-*O*-methylated feruloyl and sinapoyl malate or choline in the MOMT4 transgenic *Arabidopsis* (Zhang *et al.*, 2012). Expectedly, the similar ALDH activity and the glucose ester biosynthetic pathway might also (partially) exist in the grass species, which are able to convert the 4-*O*-methylated monolignols (and/or the corresponding aldehydes) into the corresponding 4-*O*-methylated FA and sinapte, then to the corresponding glucose esters (Supplementary Figure 8).

Tricin is the first flavonoid being recognized as an authentic lignin monomer involved in lignification in grasses (del Rio *et al.*, 2012; Lan *et al.*, 2015). It is part of the native lignin polymer in wheat (*Triticum aestivum*; (del Rio *et al.*, 2012; Zeng *et al.*, 2013), bamboo (*Phyllostachys pubescens*; Wen *et al.*, 2013, maize (*Zea mays*) (Lan *et al.*, 2016a), sugarcane (*Saccharum officinarum*; (del Río *et al.*, 2015) and rice (Lam *et al.*, 2017). Tricin incorporates into lignin polymer via 4′-*O*-β cross-coupling with normal (non-acylated) and/or acylated monolignols, and thus appears to function as a nucleation/initiation site for lignification (Lan *et al.*, 2015, 2016b, 2018). Disturbing this initiation site might alter lignin content or structure, thus affecting cell wall digestibility. Indeed, some rice mutants deficient in tricin biosynthetic genes have reduced lignin content and/or altered lignin structures with enhanced saccharification efficiency (Lam *et al.*, 2017, 2021), although the effects of the disruptions of tricin biosynthetic genes on lignin content and structure appeared to show some deviations (Lam *et al.*, 2022). The overexpression of both MOMT variants in rice resulted in notable reduction in both the methanol-soluble and lignin-bound tricin (Figures 2 and 6). Although it remains to be further determined how the expression of MOMTs suppresses tricin biosynthesis and its incorporation into lignin in transgenic rice, MOMTs exhibit discernable catalytic activities for the 4′-*O*-methyaltion of tricin and its biosynthetic precursors chrysoeriol and/or luteolin (Table 1). Such property is reminiscent of lignin biosynthetic enzyme COMTs in grass species, which has been demonstrated with dual functionality, methylating 5-hydroxyconiferaldehyde/5-hydroxyferulic acid for monolignol biosynthesis and the 3′- or 5′-hydroxyl of luteolin, tricetin, and selgin, the precursors of tricin biosynthesis (Eudes *et al.*, 2017; Kim *et al.*, 2006; Lam *et al.*, 2019; Zhou *et al.*, 2006). Interestingly, the 4′-*O*-methylated flavones were not dominantly detected in MOMT transgenic lines. Although it remains to be further determined one possibility is that the 4-*O*-methylated phenolics ferualate/sinapate resulted from disturbance of monolignol biosynthesis and/or even the trace amount of 4′-*O*-methylated flavones might act as catalytic inhibitors to the tricin biosynthetic enzymes such as OMTs thus suppressing tricin overall

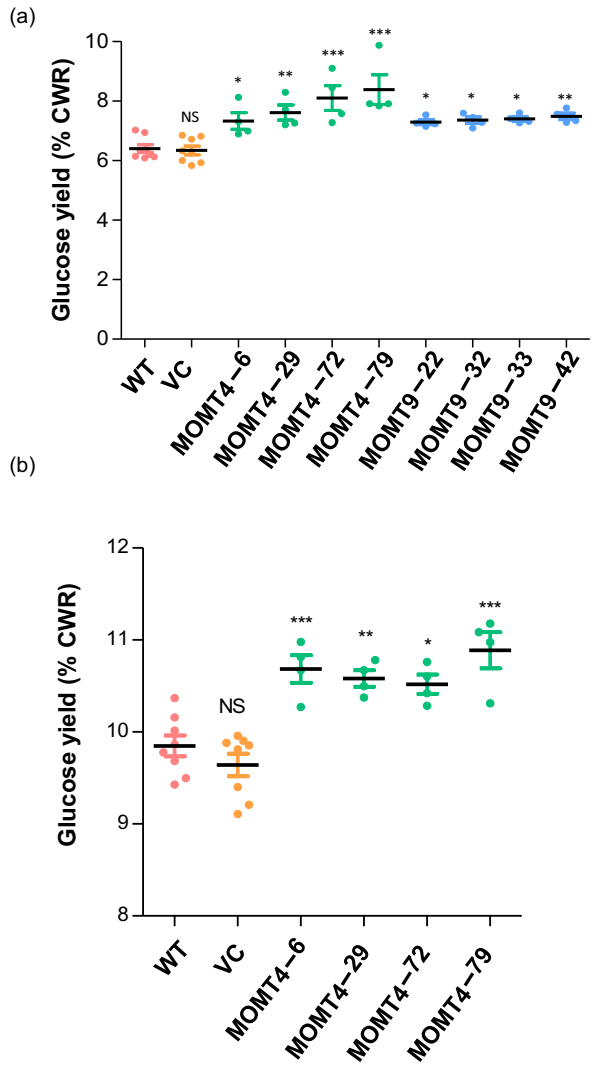

Figure 7 Digestibility of cell wall biomass from rice aerial tissues after pretreatment. (a) The amounts of glucose released from cell wall residues (CWRs) of the WT, VC, MOMT4 and MOMT9 overexpression lines following mild acid (1.2% w/v H_2SO_4) pretreatment at 30 °C for 30 min then 121 °C for 1 h and directly proceeding for cellulase digestion for 72 h. (b) The amounts of glucose released from CWRs of the WT, VC, and MOMT4 overexpression lines following mild alkaline (0.25% w/v) pretreatment at 30 °C for 30 min then 121 °C for 1 h and directly proceeding for cellulase digestion for 72 h. Data are represented as mean ± s.e. from two biological replicates with four technical repeats for the WT and VC and four technical repeats for individual MOMT4 and MOMT9 overexpression lines. * indicates statistically significant difference with $P < 0.05$; ** indicates statistically significant difference with $P < 0.01$; *** indicates statistically significant difference with $P < 0.001$ (one-way ANOVA test; Tukey's multiple comparison test). NS, not significant.

biosynthesis. This assumption apparently is consistent with the observation that accumulation levels of tricin in both the soluble fraction and lignin-bound fraction were substantially reduced in MOMT transgenic lines (Figures 2 and 6).

Engineered plants with low lignin levels have enhanced release of cell wall sugars for biofuel production (Chen and Dixon, 2007). However, modifying lignin in transgenic plants can negatively affect the growth. This phenomenon has been referred to as lignin modification-induced dwarfism (LMID), which can be attributed directly to the lack of lignin as a structural component required to support water transport, but LMID can also associate with the lack or hyperaccumulation of pathway intermediates or end products or the activation of cell wall integrity surveillance mechanisms (Muro-Villanueva *et al.*, 2019). So far, the actual cause(s) of the LMID phenotype remain unknown (Muro-Villanueva *et al.*, 2019). In the present study, both MOMT4 and MOMT9 genes were expressed in rice under the control of a strong lignin biosynthetic *C4H* gene promoter. It has been demonstrated that *C4H* promoter overperforms the constitutive cauliflower 35S promoter in driving expression cassette to manipulate lignin biosynthesis (Stewart *et al.*, 2009). The expression of MOMT4/9 resulted in substantial reduction of both G and S lignin content, the lignin-bound tricin and the wall-bound phenolics. It is not surprising that such drastic alterations in lignin biosynthesis and phenylpropanoid metabolism could render plant growth defects. The observation of more obvious dwarfism in asexually propagated transgenic offspring probably is due to the build-up of toxic phenolic substances or the accumulation of detrimental effects from generation to generation. In addition to dwarfism, MOMT4/9 transgenic lines also failed in developing viable pollen grains and consequently were sterile. It has been documented that the formation of pollen wall exine (laid by the sporopollenin precursors) and pollen intine necessarily requires the participation of phenylpropanoid metabolites such as FA, *p*CA, *p*-hydroxybenzoate and G-lignin units (Xu *et al.*, 2017; Xue *et al.*, 2020; Zhang *et al.*, 2023). The expression of MOMT4/9 driven by *OsC4H* promoter not only suppressed lignin formation but also substantially reduced cell wall FA and *p*CA. These chemical compositional changes might impair pollen wall formation thus causing the failure in pollen grain development. Previously *C4H* was shown to highly express in the tapetum layer of anthers and is involved in exine formation (Xue *et al.*, 2020). The *C4H* promoter driven MOMT gene expression might have rendered more severe disturbance on phenylpropanoid metabolism in anther tapetum layer/pollen wall. Several recent studies suggest that tailoring lignin biosynthesis in tissue- or cell type-specific manner enables to disentangle lignin modification from perturbations in plant development (De Meester *et al.*, 2018, 2021; Gui *et al.*, 2020). With validation of MOMT4/9 functioning in rice in the present study, the tissue-specific expression of MOMTs, e.g., in fibers of grasses, might be able to effectively perturb lignin biosynthesis and phenylpropanoid metabolism while mitigating the deleterious effects on plant growth.

Biomass to biofuel conversion technologies aim to access the much greater quantities of sugars in the less accessible structural carbohydrate fraction of plant biomass (Somerville, 2006), which benefits from modification of biomass chemistry (Chen and Dixon, 2007). The range of changes in lignin and wall-bound phenolics in MOMT transgenic rice resulted in a measurable improvement of saccharification of the pretreated cell wall biomass. Glucose yield from the diluted acid-treated cell wall residues of transgenic rice was enhanced up to 30% compared to the WT rice materials, which benefits the fermentable sugar-based biofuel production. Interestingly, when raw biomass of rice stem was pre-treated and digested under the same conditions, the improvement in saccharification efficiency was not easily perceived. This is probably due to the hyper-accumulation of methanol extractable 4-*O*-methylated phenolics that might be toxic to the digestive enzymes. Nevertheless, the accumulation of facile extractable phenolics in transgenic biomass could facilitate lignin valorization process and benefit the

biological upgrading of aromatics to the desired higher value end products such sustainable aviation fuels.

Materials and Methods

Generation of *MOMT4* and *MOMT9* transgenic rice

To generate *MOMT4* and *MOMT9* expression cassettes, both genes were codon optimized for grass species via GenSmart™ codon optimization program (https://www.genscript.com/tools/gensmart-codon-optimization/confirm_success) and synthesized via Genscript service with 5′ flanking sequence CACTCTGTGGTCTCATACTgcggccgcc including recognition sites of DraIII and BsaI and a Kozak sequence and 3′ flanking sequence GCTTAGAGACCACGAAGTG. An OsC4H (AC136224, LOC_Os5g25640) promoter (2kb upstream sequence before the start codon) was domesticated to fit Golden Gate/GOLDENBRAID system. Briefly, the restriction enzyme sites including BsaI, BbsI, BpiI, BsmBI, Esp3I, BtgZI and Dra III in promoter region were mutated. A sorghum SbHSP16.9 (LOC8073342) terminator was generously gifted by Fredy Altpeter's lab at University of Florida. The synthesized fragments were digested by BsaI and ligated into an intermediate construct of Golden Gate system to build the expression cassettes. Then the whole cassettes were amplified using the primers listed in Table S2 and subcloned into pCAMBIA-1302 vector using the Gibson assembly strategy. Positive clones were confirmed by restriction digestion and sequencing; then transferred into *Agrobacterium tumefaciens* EHA105 strain. Fresh calli from *Oryza sativa* cv. *Nipponbare* were transfected with *A. tumefaciens* EHA105 harbouring the designed expression cassettes following the described procedure (Nishimura *et al*., 2006).

After regeneration, the plantlets were transferred into potting soil and grew in greenhouse under a regime of 14 h light/10 h dark at 28/23 °C (day/night). For phenotyping, 1.5-month-old T_0 plants were photographed using Nikon D300 DSLR (Nikon, Japan), and their height and fresh biomass yield were measured before and after harvesting, respectively. Asexual regeneration and propagation process was adopted for successive maintenance of transgenic lines. Briefly, the young tillers of T_0 transgenic and control plants were separated and collected; then they were imbedded within moist potting soils under the same greenhouse conditions as mentioned above. After few days' incubation, new plantlets emerged from the cuttings.

Flower observation and pollen viability determination

For the pollen viability assay, spikelets were collected from the transgenic and control plants shortly before anthesis and fixed in 70% ethanol. Anthers were crushed and a drop of Lugol solution (Sigma-Aldrich) was added on the crushed anthers and were observed and photographed under Leica CTR5500 Fluorescence microscope (Leica, Germany) as per (Ranjan *et al*., 2017). Florets from the spikelets of WT and transgenic plants were manually opened with tweezer and imaged with Leica M205 FCA Fluorescence stereo microscope (Leica, Germany).

Analysis of leaf and stem soluble phenolics

For leaf soluble phenolics, approximately 100 mg of fresh leaf samples were harvested from 1.5-month-old plants and ground with cryomill (Retsch, Germany) at frequency 28 Hz for 2 min in liquid nitrogen. Soluble phenolics were extracted with 1 mL 80% methanol containing 100 μM t-*o*-coumaric acid (Sigma-Aldrich) as an internal standard in Branson 5510 ultrasonic bath (Branson, USA) for 90 min at room temperature (RT). Samples were centrifuged at 19 500 ***g*** for 15 min, twice. 1 μL of methanolic extraction was injected into an UHPLC-MS system (ThermoFisher Scientific) and resolved with a reverse phase C18 column (Luna, 150 × 2.1 mm^2, 1.6 μm, Phenomenex) as previous described gradient program and settings (Zhao *et al*., 2023). The amounts of the metabolites were quantified via measuring their peak area of UV absorbance at 330 nm or mentioned elsewhere, based on the corresponding standard curves made with authentic compounds ferulic acid, and sinapic acid run on the same UHPLC-MS system.

For stem soluble phenolics analysis, whole ariel parts including culm, leaf sheath, and leaf blades of 1.5-month-old plants were harvested and dried at 37 °C for constant weight and grounded with a Wiley® Mini-Mill (Thomas Scientific, USA) with 60 mm sieve. Approximately 10 mg powders were mixed with 500 μL of 80% methanol containing 100 μM *t-o*-coumaric acid as an internal standard and extracted as mentioned above. 5 μL of crude extracts were analysed in UHPLC-MS system as described (Zhao *et al*., 2023). For acid digestion, 250 μL of crude methanolic extracts were dried in speed vacuum (Labconco, USA), then treated with 200 μL of 2 N HCl at 90 °C for 3 h. The samples were extracted with 200 μL of water-saturated ethyl acetate containing 100 μM *t-o*-coumaric acid, twice. The extracts were dried under speed vacuum, re-dissolved in 80% methanol and centrifuged; 5 μL of the supernatant was analysed with UHPLC-MS.

Cell wall residues preparation

CWRs were prepared according to (Zhao *et al*., 2023) with slight modifications. Briefly, the weighed dry biomass were first treated with 50 mM sodium phosphate buffer (pH 7), containing 1 M NaCl and 1% Triton X100 at RT, overnight, to remove proteins. After centrifugation, the samples were extracted with 70% ethanol at 65 °C three times, chloroform: methanol (1 : 1) and acetone sequentially at RT then air-dried in laminar hood. To de-starch, the samples were treated with 90% DMSO for 24 h at RT. Further, samples were washed with 70% ethanol 7–8 times followed by acetone and air-dried in laminar hood.

Extraction and analysis of wall-bound phenolics

Alkaline hydrolysis was performed to release wall-bound phenolics (Sun *et al*., 2001). Approximately 3 mg of CWRs were dissolved in 500 μL of 4 N NaOH. Samples were incubated at 95 °C approximately for 3 h. To neutralize pH, 400 μL of 6 N HCl was added, and samples were extracted twice with 500 μL of water-saturated ethyl acetate containing 100 μM *t-o*-coumaric acid as an internal standard. The extracts were dried in a speed vacuum (Labconco, USA) and re-dissolved in 100 μL of 80% methanol. 1 μL of methanol extracts were injected into UHPLC-MS and resolved with a reverse phase C18 column (Luna, 150 × 2.1 mm^2, 1.6 μm, Phenomenex) using gradient program: 5% B (at 0 min), 30% B (at 1 min), 99% B (at 20 min), held for 7 min, then to 5% B (at 28 min) at the flow rate of 0.1 ml/min. Mobile phase A and B were 0.1% acetic acid aqueous solution and 0.1% acetic acid in acetonitrile, respectively. The compounds were detected with UV-vis diode array detector at 265, 280, 330 and 510 nm wavelengths. The amounts of the metabolites were quantified by measuring their peak area of UV absorbance at 330 nm or mentioned elsewhere.

Mild acidolysis

Mild acidolysis was performed as the described method (de Souza *et al*., 2018; Eugene *et al*., 2020; Lapierre *et al*., 2019) with slight

modifications. In brief, 10 mg of CWRs was mixed with 1 ml of 50 mM TFA (Sigma-Aldrich) and incubated at 100 °C for up to 4 h with shaking at 750 rpm. The samples were then centrifuged at 19 500 ***g***. 400 μL of supernatant was dried and re-dissolved in 100 μL of 80% methanol. 2 μL of them was analysed via UHPLC-MS (ThermoFisher Scientific) as described above. For alkaline digestion, the rest 500 μL of the TFA supernatant was dried and then treated with 2 N NaOH for 24 h at RT followed by neutralization with 6 N HCl. The samples were then extracted twice with 300 μL of water-saturated ethyl acetate containing 100 μM t-*o*-coumaric acid as the internal standard. The combined extracts were dried and resuspended in 50% methanol with 0.1% formic acid. 3 μL of each sample were analysed in UHPLC-MS as described for wall-bound phenolics.

Total lignin quantification and lignin composition analysis

Total lignin was measured by acetyl bromide method with slight modifications from (Foster *et al.*, 2010a). Briefly, 1 mL of 25% acetyl bromide (Sigma-Aldrich) was added to 4–5 mg of protein-free CWRs and incubated at 50 °C for 3 h; then the samples were cooled down on ice for 15 min and 2.5 mL of glacial acetic acid was added to stop the reaction. A volume of 400 μL 1.5 M NaOH and 300 μL of 0.5 M hydroxyl amine hydrochloride (Sigma-Aldrich) were added to 300 μL of the samples and vortexed. 200 μL of the solution was pipetted into the Corning® 96-well UV-Transparent Microplates (Corning, Kennebunk) and the absorbance was recorded at 280 nm with Spark 20M microplate reader (Tecan, Männedorf). A blank with the reagents only was included to correct background absorbance. The extinction coefficient of 17.75 g^{-1}/cm for grasses was used for the calculation of lignin content (Foster *et al.*, 2010a).

To determine the lignin monomeric composition, thioacidolysis (Rolando *et al.*, 1992) was performed with 10 mg protein-free CWRs by follow the procedure described previously (Zhao *et al.*, 2023). For derivatization, 50 μL of pyrimidine (Sigma-Aldrich) and *N*-methyl-*N*-trimethylsilyl trifluroacteamide (Sigma-Aldrich) was added and incubated for 5 h. Derivatized products were quantified with Agilent 7890A gas chromatography as described (Zhao *et al.*, 2021, 2023).

2D NMR spectroscopy

The extractive-free rice CWR samples were ball-milled with a Planetary Micro Mill Pulverisette 7 (Fritsch Industrialist) under conditions described previously (Afifi *et al.*, 2022). The ball-milled CWRs (~60 mg) were then swelled in 600 μL of dimehylsulfoxide-d_6/pyridine-d_5 (4:1; v/v) (Kim and Ralph, 2010) and subjected to the whole cell wall NMR on a Bruker Biospin Avance III 800US system (800 MHz, Bruker Biospin) equipped with a cryogenically cooled 5-mm TCI gradient probe. Adiabatic HSQC NMR experiments were performed using the standard Bruker implementation (hsqcetgpsp.3) and the parameters described previously (Kim and Ralph, 2010). Data processing and analysis were conducted using Bruker TopSpin 4.0 (Bruker Biospin) as described previously (Afifi *et al.*, 2022). Signal assignments were based on comparisons with the NMR data in literature (Afifi *et al.*, 2022; Kim and Ralph, 2010; Mansfield *et al.*, 2012; Oliveira *et al.*, 2020) as listed in Table S1. For the volume integration analysis of the whole-cell-wall spectra (Figure 6c,d), aromatic C2–H2 or C2′–H2′ correlations from lignin (**$S_{2/6}$** and **G_2**), hydroxycinnamates (**$P_{2/6}$** and **F_2**), and tricin (**$T_{2'/6'}$**) units and anomeric C1–H1 correlations from polysaccharide units (**Gl_1**, **X_1**, **X'_1**, **X''_1** and **A_1**) were manually integrated and the **$S_{2/6}$**, **$P_{2/6}$**, and **$T_{2'/6'}$** signals were logically halved. Each signal was normalized according to the sum of the integrated signals ($½S_{2/6} + G_2 + ½P_{2/6} + F_2 + ½T_{2'/6'} + Gl_1 + X_1 + X'_1 + X''_1 + A_1 = 100$).

Scanning electron microscopic imaging

For scanning electron microscopy, the fourth internode from 1.5-month-old rice plants were fixed in 2.5% glutaraldehyde in a 0.1 M sodium phosphate buffer (pH 7.0). The samples were washed with the buffer three times and cut into short segments with a vibrotome (Leica VT1000 S, Heidelberger, Germany). The stem segments were then dehydrated in a series of graded ethanol solution and dried with a Tousimis 931.GL critical-point drying apparatus (Tousimis, Rockville, MD). The samples were mounted on aluminium stubs, sputter-coated with gold, and the vibratome cutting faces were imaged at 20 kV and in high vacuum mode with a JSM-IT300LV scanning electron microscope (JEOL USA, Inc., Peabody, MA).

Cellulose content quantification

To determine crystalline cellulose content, Updegraff method (Foster *et al.*, 2010b) was employed. In brief, approximately 2 mg of CWRs was mixed with 1 ml of 2 M TFA and heated at 121 °C for 90 min and vertex every 30 min. After heating, the samples were centrifuged to separate pellets and supernatant. 1 mL of Updegraff reagent (acetic acid:nitric acid:water, 8:1:2 v/v) was added to the washed and dried pellets then heated at 100 °C for 30 min. After cooling down on ice, the samples were centrifuged at 9500 ***g*** for 15 min, the obtained pellets were washed thrice with water and once with acetone and dried overnight at RT. 172 μL of 72% sulphuric acid was added to the dried pellet and incubated at RT for 30 min. After centrifugation glucose content was determined using colorimetric anthrone assay. 200 μL freshly prepared anthrone reagent (Sigma-Aldrich) was added to 10 μL of sample in Corning® 96-well clear polystyrene microtiter plate (Corning, Kennebunk) and heated at 80 °C for 30 min. Standard curve was procured with a series of concentration of authentic glucose. Absorbance was recorded at 625 nm with Spark 20M microplate reader (Tecan, Männedorf).

The amorphous cellulose and matrix polysaccharides were measured with a phenol-sulphuric acid assay according to (Dubois *et al.*, 1956). Briefly, ~4.5 mg of CWRs were digested with 1 mL of 2 M TFA at 121 °C for 90 min. After incubation, the samples were cooled down and centrifuged at 9500 ***g*** for 10 min. 300 μL of TFA extracts was dried with a speed vacuum (Labconco), then 150 μL freshly made 5% (v/v) aqueous phenol and 1.5 mL of concentrated sulphuric acid was added and incubated at RT for 60 min. A linear response curve was procured with a series of concentration of glucose standards. Absorbance was detected with Spark 20M microplate reader (Tecan, Männedorf) at 490 nm.

Saccharification analysis

The efficiency of saccharification was determined by following the 'one-pot' method described by (Eudes *et al.*, 2012). For pretreatment, approximately 10 mg of de-starched cell wall residues and/or raw biomass samples were pretreated with either 340 μL of the dilute acid (1.2% H_2SO_4, w/v), dilute alkali (0.25% NaOH, w/v), or hot water at 30 °C for 30 min then in autoclave at 121 °C for 1 h. After that the pH was neutralized (Eudes *et al.*, 2012), then the pretreated samples were directly mixed with 650 μL of sodium citrate buffer (pH 6.2) containing 0.01%

w/v NaN_3 and 1 % w/w Cellic CTec2 cellulase (Novozymes, Denmark) to make the total volume of 1 mL and incubated at 50 °C for 72 h. After the incubation samples were centrifuged at 14 500 ***g*** for 5 min. A volume of 5 μL of the supernatant was used to quantify the released glucose using GOPOD assay kit (Megazyme, Ireland). Quadruplicate reactions were performed per plant. The data were recorded with Spark 20M microplate reader (Tecan, Männedorf) at 595 nm in Corning® 96-well clear polystyrene microtiter plate (Corning, Kennebunk). Alternatively, conventional pretreatment-digestion method was also applied to the raw biomass. Briefly, 100 mg of raw biomass was mixed with 2 mL of 4% NaOH solution and rotated at 50 °C for 2 h. Then the samples were collected and washed with water three times and kept dry at RT. The saccharification analysis was done according to (Cai *et al.*, 2016). In brief, 10 mg pretreated biomass samples were incubated with 965 μL 50 mM citric acid buffer (pH 4.8), 10 μL of 2% NaN_3 and 5 μL ACCELLERASE® 1500 (Genencor, USA) and incubated in a shaker at 50 °C for 20 h. The released glucose was determined as described above.

Enzymatic assay

The recombinant MOMT4 and MOMT9 enzymes were produced in *E. Coli* and purified via Ni-NTA affinity chromatography. After dialysis against 50 mM Tris-Cl buffer (pH 7.4) containing 150 mM NaCl, 5% glycerol and 2 mM DTT, the purified proteins were incubated in Tris-Cl buffer (pH 7.4) containing 1 mM DTT, 500 μM phenolic substrate, 500 μM SAM for 10 or 20 min at 30 °C. For monolignol and ferulic acid substrates, 5 μg of enzymes were used, while for phenolics and flavone substrates, 40 μg enzymes were employed. Products were analysed by UHPLC-MS as described in (Cai *et al.*, 2015).

Statistical analysis

For most of the experimental analyses, one-way ANOVA was used with GraphPad prism version 5 ($P \leq 0.05$, one-way ANOVA, Tukey's test). The details of statistical analyses, including the sample sizes and biological replicates, are provided in the figure legends.

Acknowledgements

We thank Dr. Fredy Altpeter at the University of Florida for generously sharing the sorghum SbHSP terminator. This work was primarily funded by the DOE Center for Advanced Bioenergy and Bioproducts Innovation (U.S. Department of Energy, Office of Science, Office of Biological and Environmental Research under Award Number DE-C0018420). Any opinions, findings and conclusions or recommendations expressed in this publication are those of the author(s) and do not necessarily reflect the views of the U.S. Department of Energy. The enzyme characterization and saccharification analysis were partially supported by the Joint BioEnergy Institute, one of the Bioenergy Research Centers of the US DOE, Office of Science, Office of Biological and Environmental Research, through contract DE-AC02-05CH11231 between the Lawrence Berkeley National Laboratory and the US DOE. Cell wall chemical analyses were partially supported by the DOE, Office of Science, Office of Basic Energy Sciences, especially the Physical Biosciences program of the Chemical Sciences, Geosciences and Biosciences Division under contract no. DE-SC0012704 (to C.-J.L.). S.Y. and Y.T. acknowledge the research grants from the Japan Society for the Promotion of Science (grant no. JP20H03044 and JP 22J13457). A part of the study was conducted using the facilities in the DASH/FBAS of RISH, Kyoto University and the NMR spectrometer at the JURC of ICR, Kyoto University.

Conflict of interest

The authors declared that they do not have conflicts of interest.

Author contributions

C.-J.L. and N.D. conceived the research plan and designed the experiments. N.D. constructed the expression cassette, conducted rice transformation and physiological and chemical analyses on transgenic plants. N.D. and F.B. performed the enzyme activity assay. Y.Z. conducted the saccharification assessment. G. H conducted histochemical and SEM imaging. S.Y. and Y.T. conducted NMR analysis. C.-J. L. coordinated the project. C.-J.L., N.D., Y.Z., S.Y. and Y.T. analysed and interpreted data. C.-J.L. and N.D. prepared the manuscript. All the authors edited the manuscript and approved the final version of the manuscript.

References

Afifi, O.A., Tobimatsu, Y., Lam, P.Y., Martin, A.F., Miyamoto, T., Osakabe, Y., Osakabe, K. *et al.* (2022) Genome-edited rice deficient in two *4-COUMARATE:COENZYME A LIGASE* genes displays diverse lignin alterations. *Plant Physiol.* **190**, 2155–2172.

Bartley, L.E., Peck, M.L., Kim, S.R., Ebert, B., Manisseri, C., Chiniquy, D.M., Sykes, R. *et al.* (2013) Overexpression of a BAHD acyltransferase, *OsAt10*, alters rice cell wall hydroxycinnamic acid content and saccharification. *Plant Physiol.* **161**, 1615–1633.

Bhuiya, M.W. and Liu, C.J. (2010) Engineering monolignol 4-*O*-methyltransferases to modulate lignin biosynthesis. *J. Biol. Chem.* **285**, 277–285.

Bunzel, M., Ralph, J., Lu, F., Hatfield, R.D. and Steinhart, H. (2004) Lignins and ferulate-coniferyl alcohol cross-coupling products in cereal grains. *J. Agric. Food Chem.* **52**, 6496–6502.

Cai, Y., Bhuiya, M.W., Shanklin, J. and Liu, C.J. (2015) Engineering a monolignol 4-*O*-methyltransferase with high selectivity for the condensed lignin precursor coniferyl alcohol. *J. Biol. Chem.* **290**, 26715–26724.

Cai, Y., Zhang, K., Kim, H., Hou, G., Zhang, X., Yang, H., Feng, H. *et al.* (2016) Enhancing digestibility and ethanol yield of Populus wood via expression of an engineered monolignol 4-*O*-methyltransferase. *Nat. Commun.* **7**, 11989.

Chen, F. and Dixon, R.A. (2007) Lignin modification improves fermentable sugar yields for biofuel production. *Nat. Biotechnol.* **25**, 759–761.

Coomey, J.H., Sibout, R. and Hazen, S.P. (2020) Grass secondary cell walls, *Brachypodium distachyon* as a model for discovery. *New Phytol.* **227**, 1649–1667.

Davin, L.B. and Lewis, N.G. (2005) Lignin primary structures and dirigent sites. *Curr. Opin. Biotechnol.* **16**, 407–415.

De Meester, B., de Vries, L., Ozparpucu, M., Gierlinger, N., Corneillie, S., Pallidis, A., Goeminne, G. *et al.* (2018) Vessel-specific reintroduction of *CINNAMOYL-COA REDUCTASE1 (CCR1)* in Dwarfed *ccr1* mutants restores vessel and Xylary fiber integrity and increases biomass. *Plant Physiol.* **176**, 611–633.

De Meester, B., Vanholme, R., de Vries, L., Wouters, M., Van Doorsselaere, J. and Boerjan, W. (2021) Vessel- and ray-specific monolignol biosynthesis as an approach to engineer fiber-hypolignification and enhanced saccharification in poplar. *Plant J.* **108**, 752–765.

Dubois, M., Gilles, K.A., Hamilton, J.K., Rebers, P.A. and Smith, F. (1956) Colorimetric method for determination of sugars and related substances. *Anal. Chem.* **28**, 350–356.

Eudes, A., George, A., Mukerjee, P., Kim, J.S., Pollet, B., Benke, P.I., Yang, F. *et al.* (2012) Biosynthesis and incorporation of side-chain-truncated lignin monomers to reduce lignin polymerization and enhance saccharification. *Plant Biotechnol. J.* **10**, 609–620.

Eudes, A., Dutta, T., Deng, K., Jacquet, N., Sinha, A., Benites, V.T., Baidoo, E.E.K. *et al*. (2017) *SbCOMT (Bmr12)* is involved in the biosynthesis of tricin-lignin in sorghum. *PLoS One* **12**, e0178160.

Eugene, A., Lapierre, C. and Ralph, J. (2020) Improved analysis of arabinoxylan-bound hydroxycinnamate conjugates in grass cell walls. *Biotechnol. Biofuels* **13**, 202.

Fornale, S., Rencoret, J., Garcia-Calvo, L., Encina, A., Rigau, J., Gutierrez, A., Del Rio, J.C. *et al*. (2017) Changes in cell wall polymers and degradability in maize mutants lacking 3′- and 5′-*O*-methyltransferases involved in lignin biosynthesis. *Plant Cell Physiol.* **58**, 240–255.

Foster, C.E., Martin, T.M. and Pauly, M. (2010a) Comprehensive compositional analysis of plant cell walls (lignocellulosic biomass) part I: lignin. *J. Vis. Exp.* **11**, 1745.

Foster, C.E., Martin, T.M. and Pauly, M. (2010b) Comprehensive compositional analysis of plant cell walls (lignocellulosic biomass) part II: carbohydrates. *J. Vis. Exp.* **12**, 1837.

Grabber, J.H., Ralph, J. and Hatfield, R.D. (1998) Ferulate cross-links limit the enzymatic degradation of synthetically lignified primary walls of maize. *J. Agric. Food Chem.* **46**, 2609–2614.

Gui, J., Lam, P.Y., Tobimatsu, Y., Sun, J., Huang, C., Cao, S., Zhong, Y. *et al*. (2020) Fibre-specific regulation of lignin biosynthesis improves biomass quality in Populus. *New Phytol.* **226**, 1074–1087.

Guo, D., Chen, F., Wheeler, J., Winder, J., Selman, S., Peterson, M. and Dixon, R.A. (2001) Improvement of in-rumen digestibility of alfalfa forage by genetic manipulation of lignin *O*-methyltransferases. *Transgenic Res.* **10**, 457–464.

Halpin, C. (2019) Lignin engineering to improve saccharification and digestibility in grasses. *Curr. Opin. Biotechnol.* **56**, 223–229.

Hatfield, R.D., Ralph, J. and Grabber, J.H. (1999) Cell wall cross-linking by ferulates and diferulates in grasses. *J. Sci. Food Agric.* **79**, 403–407.

Hatfield, R.D., Rancour, D.M. and Marita, J.M. (2016) Grass cell walls: a story of cross-Linking. *Front. Plant Sci.* **7**, 2056.

Karlen, S.D., Zhang, C., Peck, M.L., Smith, R.A., Padmakshan, D., Helmich, K.E., Free, H.C. *et al*. (2016) Monolignol ferulate conjugates are naturally incorporated into plant lignins. *Sci. Adv.* **2**, e1600393.

Karlen, S.D., Free, H.C.A., Padmakshan, D., Smith, B.G., Ralph, J. and Harris, P.J. (2018) Commelinid monocotyledon lignins are acylated by *p*-coumarate. *Plant Physiol.* **177**, 513–521.

Kim, S. and Dale, B.E. (2004) Global potential bioethanol production from wasted crops and crop residues. *Biomass Bioenerg.* **26**, 361–375.

Kim, H. and Ralph, J. (2010) Solution-state 2D NMR of ball-milled plant cell wall gels in DMSO-d(6)/pyridine-d(5). *Org. Biomol. Chem.* **8**, 576–591.

Kim, B.G., Lee, Y., Hur, H.G., Lim, Y. and Ahn, J.H. (2006) Flavonoid 3′-*O*-methyltransferase from rice: cDNA cloning, characterization and functional expression. *Phytochemistry* **67**, 387–394.

Kosel, J., Vizintin, L., Majer, A. and Bohanec, B. (2018) Staining for viability testing, germination and maturation of *Sambucus nigra* L. pollen in vitro. *Biotech. Histochem.* **93**, 1–9.

Lam, P.Y., Tobimatsu, Y., Takeda, Y., Suzuki, S., Yamamura, M., Umezawa, T. and Lo, C. (2017) Disrupting *Flavone Synthase II* alters lignin and improves biomass digestibility. *Plant Physiol.* **174**, 972–985.

Lam, P.Y., Tobimatsu, Y., Matsumoto, N., Suzuki, S., Lan, W., Takeda, Y., Yamamura, M. *et al*. (2019) *OsCAldOMT1* is a bifunctional *O*-methyltransferase involved in the biosynthesis of tricin-lignins in rice cell walls. *Sci. Rep.* **9**, 11597.

Lam, P.Y., Lui, A.C.W., Wang, L.X., Liu, H.J., Umezawa, T., Tobimatsu, Y. and Lo, C. (2021) Tricin biosynthesis and bioengineering. *Front. Plant Sci.* **12**, 733198.

Lam, P.Y., Wang, L., Lui, A.C.W., Liu, H., Takeda-Kimura, Y., Chen, M.-X., Zhu, F.-Y. *et al*. (2022) Deficiency in flavonoid biosynthesis genes CHS, CHI and CHIL alters rice flavonoid and lignin profiles. *Plant Physiol*, **188**, 1993–2011.

Lan, W., Lu, F., Regner, M., Zhu, Y., Rencoret, J., Ralph, S.A., Zakai, U.I. *et al*. (2015) Tricin, a flavonoid monomer in monocot lignification. *Plant Physiol.* **167**, 1284–1295.

Lan, W., Morreel, K., Lu, F., Rencoret, J., Carlos Del Rio, J., Voorend, W., Vermerris, W. *et al*. (2016a) Maize tricin-oligolignol metabolites and their implications for monocot lignification. *Plant Physiol.* **171**, 810–820.

Lan, W., Rencoret, J., Lu, F., Karlen, S.D., Smith, B.G., Harris, P.J., Del Rio, J.C. *et al*. (2016b) Tricin-lignins: occurrence and quantitation of tricin in relation to phylogeny. *Plant J.* **88**, 1046–1057.

Lan, W., Yue, F., Rencoret, J., Del Rio, J.C., Boerjan, W., Lu, F. and Ralph, J. (2018) Elucidating tricin-lignin structures: assigning correlations in HSQC spectra of monocot lignins. *Polymers (Basel)* **10**, 916.

Lapierre, C., Voxeur, A., Boutet, S. and Ralph, J. (2019) Arabinose conjugates diagnostic of ferulate-ferulate and ferulate-monolignol cross-coupling are released by mild acidolysis of grass cell walls. *J. Agric. Food Chem.* **67**, 12962–12971.

Li, G., Jones, K.C., Eudes, A., Pidatala, V.R., Sun, J., Xu, F., Zhang, C. *et al*. (2018) Overexpression of a rice *BAHD* acyltransferase gene in switchgrass (*Panicum virgatum* L.) enhances saccharification. *BMC Biotechnol.* **18**, 54.

Liu, C.J. and Cai, Y. (2017) *Specialized (iso)eugenol-4-O-methyltransferases (s-IEMTs) and methods of making and using the same. (office, U.S.P. ed)*. United States: Brookhaven Science Associates, LLC, Upton, NY (US).

Liu, C.J., Cai, Y., Zhang, X., Gou, M. and Yang, H. (2014) Tailoring lignin biosynthesis for efficient and sustainable biofuel production. *Plant Biotechnol. J.* **12**, 1154–1162.

Mansfield, S.D., Kim, H., Lu, F. and Ralph, J. (2012) Whole plant cell wall characterization using solution-state 2D NMR. *Nat. Protoc.* **7**, 1579–1589.

Moore, K.J. and Jung, H. (2001) Lignin and fiber digestion. *J. Range Manag.* **54**, 420–430.

Muro-Villanueva, F., Mao, X. and Chapple, C. (2019) Linking phenylpropanoid metabolism, lignin deposition, and plant growth inhibition. *Curr. Opin. Biotechnol.* **56**, 202–208.

Nair, R.B., Bastress, K.L., Ruegger, M.O., Denault, J.W. and Chapple, C. (2004) The *Arabidopsis thaliana REDUCED EPIDERMAL FLUORESCENCE1* gene encodes an aldehyde dehydrogenase involved in ferulic acid and sinapic acid biosynthesis. *Plant Cell* **16**, 544–554.

Nishimura, A., Aichi, I. and Matsuoka, M. (2006) A protocol for Agrobacterium-mediated transformation in rice. *Nat. Protoc.* **1**, 2796–2802.

de Oliveira, D.M., Finger-Teixeira, A., Mota, T.R., Salvador, V.H., Moreira-Vilar, F.C., Molinari, H.B., Mitchell, R.A. *et al*. (2015) Ferulic acid: a key component in grass lignocellulose recalcitrance to hydrolysis. *Plant Biotechnol. J.* **13**, 1224–1232.

Oliveira, D.M., Mota, T.R., Salatta, F.V., Sinzker, R.C., Koncitikova, R., Kopecny, D., Simister, R. *et al*. (2020) Cell wall remodeling under salt stress: insights into changes in polysaccharides, feruloylation, lignification, and phenolic metabolism in maize. *Plant Cell Environ.* **43**, 2172–2191.

Osakabe, K., Tsao, C.C., Li, L., Popko, J.L., Umezawa, T., Carraway, D.T., Smeltzer, R.H. *et al*. (1999) Coniferyl aldehyde 5-hydroxylation and methylation direct syringyl lignin biosynthesis in angiosperms. *Proc. Natl. Acad. Sci. USA* **96**, 8955–8960.

Parvathi, K., Chen, F., Guo, D., Blount, J.W. and Dixon, R.A. (2001) Substrate preferences of *O*-methyltransferases in alfalfa suggest new pathways for 3-*O*-methylation of monolignols. *Plant J.* **25**, 193–202.

Petrik, D.L., Karlen, S.D., Cass, C.L., Padmakshan, D., Lu, F., Liu, S., Le Bris, P. *et al*. (2014) *p*-Coumaroyl-CoA:monolignol transferase (PMT) acts specifically in the lignin biosynthetic pathway in *Brachypodium distachyon*. *Plant J.* **77**, 713–726.

Ralph, J., Grabber, J.H. and Hatfield, R.D. (1995) Lignin-ferulate cross-links in grasses: active incorporation of ferulate polysaccharide esters into ryegrass lignins. *Carbohydr. Res.* **275**, 167–178.

Ralph, J., Guillaumie, S., Grabber, J.H., Lapierre, C. and Barriere, Y. (2004) Genetic and molecular basis of grass cell-wall biosynthesis and degradability. III. Towards a forage grass ideotype. *C. R. Biol.* **327**, 467–479.

Ralph, J., Lapierre, C. and Boerjan, W. (2019) Lignin structure and its engineering. *Curr. Opin. Biotechnol.* **56**, 240–249.

Ranjan, R., Khurana, R., Malik, N., Badoni, S., Parida, S.K., Kapoor, S. and Tyagi, A.K. (2017) bHLH142 regulates various metabolic pathway-related genes to affect pollen development and anther dehiscence in rice. *Sci. Rep.* **7**, 43397.

del Rio, J.C., Rencoret, J., Prinsen, P., Martinez, A.T., Ralph, J. and Gutierrez, A. (2012) Structural characterization of wheat straw lignin as revealed by analytical pyrolysis, 2D-NMR, and reductive cleavage methods. *J. Agric. Food Chem.* **60**, 5922–5935.

del Río, J.C., Lino, A.G., Colodette, J.L., Lima, C.F., Gutiérrez, A., Martínez, Á.T., Lu, F. *et al*. (2015) Differences in the chemical structure of the lignins from sugarcane bagasse and straw. *Biomass Bioenerg.* **81**, 322–338.

Rolando, C., Monties, B. and Lapierre, C. (1992) Thioacidolysis. In *Methods in Lignin Chemistry*(Lin, S.Y. and Dence, C.W., eds), pp. 334–349. Berlin, Heidelberg: Springer Berlin Heidelberg.

Somerville, C. (2006) Biofuel. *Curr. Biol.* **17**, R115–R119.
de Souza, W.R., Martins, P.K., Freeman, J., Pellny, T.K., Michaelson, L.V., Sampaio, B.L., Vinecky, F. *et al*. (2018) Suppression of a single *BAHD* gene in Setaria viridis causes large, stable decreases in cell wall feruloylation and increases biomass digestibility. *New Phytol.* **218**, 81–93.
Stewart, J.J., Akiyama, T., Chapple, C., Ralph, J. and Mansfield, S.D. (2009) The effects on lignin structure of overexpression of ferulate 5-hydroxylase in hybrid poplar. *Plant Physiol.* **150**, 621–635.
Sun, R.C., Sun, X.F. and Zhang, S.H. (2001) Quantitative determination of hydroxycinnamic acids in wheat, rice, rye, and barley straws, maize stems, oil palm frond fiber, and fast-growing poplar wood. *J. Agric. Food Chem.* **49**, 5122–5129.
Tobimatsu, Y. and Schuetz, M. (2019) Lignin polymerization: how do plants manage the chemistry so well? *Curr. Opin. Biotechnol.* **56**, 75–81.
Tye, Y.Y., Lee, K.T., Wan Abdullah, W.N. and Leh, C.P. (2016) The world availability of non-wood lignocellulosic biomass for the production of cellulosic ethanol and potential pretreatments for the enhancement of enzymatic saccharification. *Renew. Sust. Energ. Rev.* **60**, 155–172.
Umezawa, T. (2018) Lignin modification in planta for valorization. *Phytochem. Rev.* **17**, 1305–1327.
Vanholme, R., Demedts, B., Morreel, K., Ralph, J. and Boerjan, W. (2010) Lignin biosynthesis and structure. *Plant Physiol.* **153**, 895–905.
Wen, J.-L., Sun, S.-L., Xue, B.-L. and Sun, R.-C. (2013) Quantitative structural characterization of the lignins from the stem and pith of bamboo (*Phyllostachys pubescens*). *Holzforschung* **6**, 613–627.
Withers, S., Lu, F., Kim, H., Zhu, Y., Ralph, J. and Wilkerson, C.G. (2012) Identification of grass-specific enzyme that acylates monolignols with *p*-coumarate. *J. Biol. Chem.* **287**, 8347–8355.
Xu, D., Shi, J., Rautengarten, C., Yang, L., Qian, X., Uzair, M., Zhu, L. *et al*. (2017) Defective pollen wall 2 (DPW2) encodes an acyl transferase required for rice pollen development. *Plant Physiol.* **173**, 240–255.
Xue, J.S., Zhang, B., Zhan, H., Lv, Y.L., Jia, X.L., Wang, T., Yang, N.Y. *et al*. (2020) Phenylpropanoid derivatives are essential components of sporopollenin in vascular plants. *Mol. Plant* **13**, 1644–1653.
Zeng, J., Helms, G.L., Gao, X. and Chen, S. (2013) Quantification of wheat straw lignin structure by comprehensive NMR analysis. *J. Agric. Food Chem.* **61**, 10848–10857.
Zhang, K., Bhuiya, M.W., Pazo, J.R., Miao, Y., Kim, H., Ralph, J. and Liu, C.J. (2012) An engineered monolignol 4-*O*-methyltransferase depresses lignin biosynthesis and confers novel metabolic capability in Arabidopsis. *Plant Cell* **24**, 3135–3152.
Zhang, L., Zheng, L., Wu, J., Liu, Y., Liu, W., He, G. and Wang, N. (2023) *OsCCRL1* is essential for phenylpropanoid metabolism in rice anthers. *Rice (N Y)* **16**, 10.
Zhao, Y., Yu, X., Lam, P.Y., Zhang, K., Tobimatsu, Y. and Liu, C.J. (2021) Monolignol acyltransferase for lignin *p*-hydroxybenzoylation in Populus. *Nat. Plants* **7**, 1288–1300.
Zhao, X., Zhao, Y., Gou, M. and Liu, C.J. (2023) Tissue-preferential recruitment of electron transfer chains for cytochrome P450-catalyzed phenolic biosynthesis. *Sci. adv.* **9**, eade4389.
Zhou, J.-M., Fukushi, Y., Wang, X.-f. and Ibrahim, R.K. (2006) Characterization of a novel *Flavone O-Methyltransferase* gene in rice. *Nat. Prod. Commun.* **1**, 981–984.

Supporting information

Additional supporting information may be found online in the Supporting Information section at the end of the article.

Figure S1 Phenotypic analysis of MOMT4 and MOMT9 over-expression plants after the fourth successive asexual regeneration.
Figure S2 Structure characterization of the methanol soluble phenolics from rice aerial tissues.
Figure S3 The methanol extractable phenolics from rice leaf tissues.
Figure S4 UV-LC-MS-based characterization of the mild acid-olysis products from cell wall residues of rice aerial tissues.
Figure S5 Two-dimensional NMR spectra of whole stem cell walls from the wild type (WT), empty vector control (VC), MOMT4 and MOMT9 transgenic rice plants.
Figure S6 Cellulosic sugar content in MOMT transgenic plants.
Figure S7 Saccharification analysis of raw biomass of MOMT transgenic plants.
Figure S8 Summary of the effects of the overexpression of MOMT4/9 in transgenic rice on lignin biosynthesis and phenyl-propanoid metabolism.
Table S1 Peak assignments for 2D HSQC NMR spectra of rice cell walls.
Table S2 The primers used in this study.